RESEARCH ARTICLE

Virus-Encoded MicroRNAs Facilitate Gammaherpesvirus Latency and Pathogenesis *In Vivo*

Emily R. Feldman,[a] Mehmet Kara,[a] Carrie B. Coleman,[a] Katrina R. Grau,[a] Lauren M. Oko,[b] Brian J. Krueger,[a] Rolf Renne,[a] Linda F. van Dyk,[b] Scott A. Tibbetts[a]

Department of Molecular Genetics & Microbiology and UF Shands Cancer Center, College of Medicine, University of Florida, Gainesville, Florida, USA[a]; Departments of Microbiology and Immunology, University of Colorado School of Medicine, Aurora, Colorado, USA[b]

ABSTRACT **Gammaherpesviruses, including Epstein-Barr virus (EBV), Kaposi sarcoma-associated herpesvirus (KSHV, or HHV-8), and murine gammaherpesvirus 68 (MHV68, γHV68, or MuHV-4), are B cell-tropic pathogens that each encode at least 12 microRNAs (miRNAs). It is predicted that these regulatory RNAs facilitate infection by suppressing host target genes involved in a wide range of key cellular pathways. However, the precise contribution that gammaherpesvirus miRNAs make to viral life cycle and pathogenesis *in vivo* is unknown. MHV68 infection of mice provides a highly useful system to dissect the function of specific viral elements in the context of both asymptomatic infection and disease. Here, we report (i) analysis of *in vitro* and *in vivo* MHV68 miRNA expression, (ii) generation of an MHV68 miRNA mutant with reduced expression of all 14 pre-miRNA stem-loops, and (iii) comprehensive phenotypic characterization of the miRNA mutant virus *in vivo*. The profile of MHV68 miRNAs detected in infected cell lines varied with cell type and did not fully recapitulate the profile from cells latently infected *in vivo*. The miRNA mutant virus, MHV68.Zt6, underwent normal lytic replication *in vitro* and *in vivo*, demonstrating that the MHV68 miRNAs are dispensable for acute replication. During chronic infection, MHV68.Zt6 was attenuated for latency establishment, including a specific defect in memory B cells. Finally, MHV68.Zt6 displayed a striking attenuation in the development of lethal pneumonia in mice deficient in IFN-γ. These data indicate that the MHV68 miRNAs may facilitate virus-driven maturation of infected B cells and implicate the miRNAs as a critical determinant of gammaherpesvirus-associated disease.**

IMPORTANCE **Gammaherpesviruses such as EBV and KSHV are widespread pathogens that establish lifelong infections and are associated with the development of numerous types of diseases, including cancer. Gammaherpesviruses encode many small noncoding RNAs called microRNAs (miRNAs). It is predicted that gammaherpesvirus miRNAs facilitate infection and disease by suppressing host target transcripts involved in a wide range of key cellular pathways; however, the precise contribution that these regulatory RNAs make to *in vivo* virus infection and pathogenesis is unknown. Here, we generated a mutated form of murine gammaherpesvirus (MHV68) to dissect the function of gammaherpesvirus miRNAs *in vivo*. We demonstrate that the MHV68 miRNAs were dispensable for short-term virus replication but were important for establishment of lifelong infection in the key virus reservoir of memory B cells. Moreover, the MHV68 miRNAs were essential for the development of virus-associated pneumonia, implicating them as a critical component of gammaherpesvirus-associated disease.**

Received 21 February 2014 **Accepted** 24 April 2014 **Published** 27 May 2014

Citation Feldman ER, Kara M, Coleman CB, Grau KR, Oko LM, Krueger BJ, Renne R, van Dyk LF, Tibbetts SA. 2014. Virus-encoded microRNAs facilitate gammaherpesvirus latency and pathogenesis *in vivo*. mBio 5(3):e00981-14. doi:10.1128/mBio.00981-14.

Editor Rozanne Sandri-Goldin, University of California, Irvine

Address correspondence to Scott A. Tibbetts, stibbe@ufl.edu.

Gammaherpesviruses, such as the human pathogens Kaposi sarcoma-associated herpesvirus (KSHV, or HHV-8) and Epstein-Barr virus (EBV), as well as the murine gammaherpesvirus 68 (MHV68, MuHV-4, or γHV68), are lymphotropic viruses characterized by their ability to establish lifelong infections within their host. Furthermore, gammaherpesviruses have a consequent association with the development of a variety of malignancies, including B cell lymphomas and Kaposi's sarcoma (1–3). These viruses have also been linked to an assortment of other diseases, including posttransplant complications, large-vessel vasculitis, autoimmunity, and lethal pneumonia. Following initial colonization of the host and virus amplification during the acute phase of infection, gammaherpesviruses establish chronic infection in a limited fraction of lymphoid cells. In particular, circulating mature B cells have been identified as a primary reservoir of latent infection for KSHV, EBV, and MHV68 (4–9).

Central to the process of chronic gammaherpesvirus infection is the establishment of a highly restricted viral gene expression program within the infected cells, which enables these viruses to evade continuous active immune surveillance and persist *in vivo* throughout the lifetime of the host. One component of this restricted program is the transcription of noncoding RNAs (ncRNAs), such as microRNAs (miRNAs) (10, 11). These ~22-nucleotide miRNAs typically bind imperfectly to the 3′ untranslated region (UTR) of target mRNAs and regulate protein expression through mechanisms involving mRNA degradation,

sequestration, and translational repression (12). Mammalian miRNAs are known to participate in cell differentiation, metabolism, homeostasis, apoptosis, and cancer. Therefore, not surprisingly, it has recently been reported that many viruses, including the herpesviruses, polyomaviruses and some retroviruses, have adopted miRNAs as a means to promote viral fitness (13–16). EBV and KSHV encode 25 and 12 pre-miRNAs, respectively (10, 11, 17–20). Potential targets of EBV and KSHV miRNAs have been identified through experiments utilizing cross-linking immunoprecipitation (CLIP) of RNA-induced silencing complexes (RISC) from cultured human tumor cell lines (21–25). Such experiments, in conjunction with molecular target validation and biological significance studies, have demonstrated that EBV and KSHV miRNAs target transcripts are involved in immune recognition, apoptosis, and cell cycle pathways, among others (16, 26). Recent studies have also demonstrated that at least some gammaherpesvirus miRNAs can act as functional orthologs of host miRNAs. For example, KSHV miR-K12-11 shares seed homology with hsa-miR-155 (27, 28), and can similarly induce B cell differentiation and expansion (29, 30). Interestingly, some viral ncRNAs may also regulate the expression of host miRNAs, including regulatory RNAs involved in lymphocyte activation and maturation (31). Finally, several viral miRNAs directly suppress specific viral transcripts, perhaps in part as a mechanism to fine-tune leaky transcription during persistent infections (13).

Thus, emerging evidence indicates that gammaherpesvirus miRNAs target both virus and host transcripts. However, the *in vivo* functions of these regulatory RNAs remain elusive. Whereas studies of the human gammaherpesviruses EBV and KSHV have been confined primarily to *in vitro* studies by the narrow host range of these viruses, MHV68 provides a small-animal model for refining the study of molecular and cellular events that occur during gammaherpesvirus latency and pathogenesis (32). MHV68 is a murine gammaherpesvirus originally isolated from a free-living rodent population (33, 34). Like the human gammaherpesviruses, MHV68 establishes long-term latency in B cells and is capable of inducing lymphoma and lymphoproliferative disease (6, 35, 36). Like EBV and KSHV, MHV68 encodes miRNAs, which were identified by small-RNA cloning and deep-sequencing approaches. Now, 15 MHV68 mature miRNAs have been detected, all of which are clustered at the 5′ end of the genome (11, 37–39). Uniquely, all MHV68 miRNAs are located downstream of viral tRNA-like elements (vtRNAs) and transcribed by RNA polymerase III from canonical polymerase III promoters. These linked tRNA-miRNA-encoding RNAs (TMERs) harbor one or two miRNA-containing stem-loops each and are initially cleaved by tRNaseZ instead of Drosha, similar to cellular noncoding tRNAs (40, 41). Interestingly, even prior to the discovery of small regulatory ncRNAs in mammals, early MHV68 studies demonstrated high expression levels of these vtRNA-linked transcripts in latently infected cells during asymptomatic infection, as well as in proliferating B cells in the context of lymphoproliferative disease (36, 42). Thus, these TMER transcripts are highly expressed as a normal process of the *in vivo* biology of MHV68. However, the function of the MHV68 TMERs and all gammaherpesvirus-encoded miRNAs during *in vivo* infection is poorly understood.

To better define the biological role of MHV68-encoded miRNAs *in vivo*, we have (i) quantified the relative expression levels of mature miRNAs during various phases of infection, (ii) generated an MHV68 mutant virus with completely absent or significantly reduced expression of all 14 pre-miRNAs, and (iii) tested the ability of this mutant to undergo acute replication, establish latency, and cause disease. In this paper, we demonstrate that the MHV68-encoded miRNAs are expressed at high levels throughout the acute phase of infection *in vitro* and in latently infected cells *in vivo*. Interestingly, the patterns of expression during *in vivo* latency differed from that previously reported for latent cell lines. Furthermore, although the MHV68 miRNAs were completely dispensable for acute replication, they altered the establishment of latency in specific B cell subsets. Finally, a lack of miRNA expression resulted in the complete attenuation of lethal disease in a virus-induced pneumonia model, demonstrating a key role for the viral miRNAs in gammaherpesvirus pathogenesis.

RESULTS

MHV68 miRNA and TMER nomenclature. Several previous reports identified mature virus-encoded miRNAs (see Table S1 in the supplemental material) expressed in cells infected with MHV68 *in vitro* (11, 37, 38, 41, 43). Because these studies were published independently, several identical or overlapping sequences have been assigned different names by each research group. Some but not all of these sequences have been reported in the online microRNA database miRBase (http://www.mirbase.org/) (44). Additionally, in some cases, there remains ambiguity about whether the biologically relevant miRNA corresponds to (i) the annotated sequence itself, (ii) a sequence that is shifted by 1 to 4 nucleotides, or (iii) the miRNA(*) sequence on the opposing strand. For example, sequences corresponding to the stem-loop strand opposing the previously annotated mghv-miR-M1-2 have been detected more frequently than sequences for the annotated miR-M1-2 itself (37, 38). To consolidate and clarify the annotation of MHV68-encoded miRNAs we, along with Diebel et al. (K. W. Diebel, L. M. Oko, E. M. Medina, C. J. Warren, B. F. Niemeyer, D. J. Claypool, S. A. Tibbetts, C. D. Cool, E. T. Clambey, L. F. van Dyk, submitted for publication), propose an updated nomenclature system (Fig. 1; also, see Table S1 in the supplemental material). This system retains the current association of miRbase numbering with *in silico*-predicted pre-miRNA stem-loops but assigns miRNA names based on stem-loop strands rather than specific confirmed miRNA sequences. For example, the current miRBase entry "mghv-miR-M1-1," which is located on the 3p strand of the first stem-loop downstream of vtRNA1 (Fig. 1), would instead be named "mghv-miR-M1-1-3p." Thus, in this nomenclature system, (i) "TMER1" refers to the entire vtRNA-linked transcript (vtRNA1-pre-miR-1-pre-miR-10); (ii) "mghv-miR-M1-1" refers to the entire upstream stem-loop, which encodes the potential miRNAs miR-M1-1-5p and miR-M1-1-3p; and (iii) "mghv-miR-M1-10" refers to the entire downstream stem-loop, which encodes the potential miRNAs miR-M1-10-5p and miR-M1-10-3p. For the purpose of clarity, the new nomenclature system is used in this article.

Expression of MHV68-encoded miRNAs is dependent upon cell type and state of infection. As described above, previous studies of miRNA expression utilized small-RNA cloning and deep-sequencing techniques to identify MHV68-encoded miRNAs in lytically infected fibroblasts and latently infected or reactivated S11 B cells. To further refine our understanding of MHV68 miRNA expression, including the kinetics and relative levels of expression during various phases of infection, we performed quantitative TaqMan PCR using stem-loop RT primers and probe

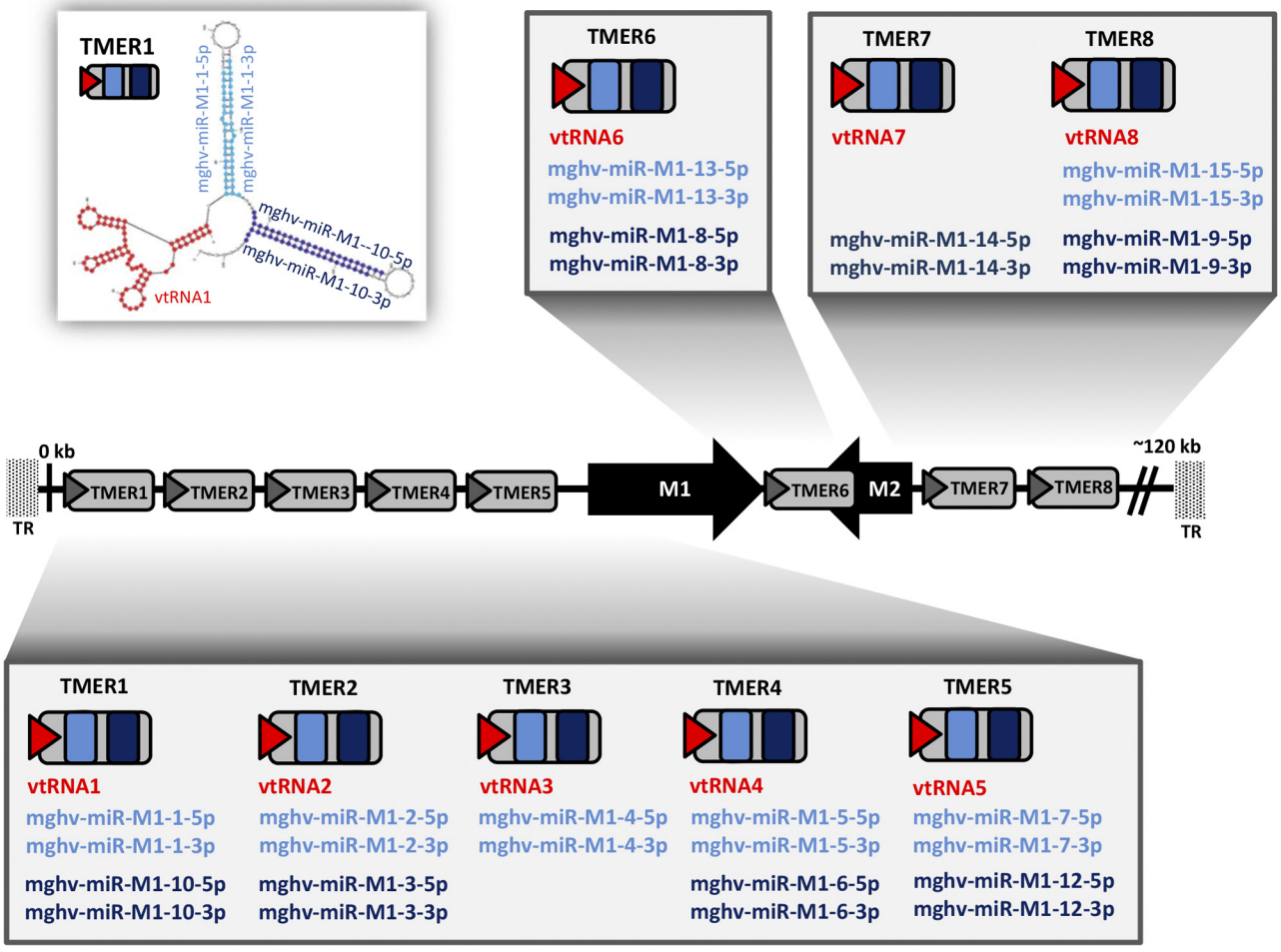

FIG 1 Proposed MHV68-encoded miRNA and TMER nomenclature. The diagram depicts approximately 6 kb of the 5′ end of the MHV68 genome, which includes eight tRNA-miRNA-encoding RNA (TMER) genes and two unique M genes. Each TMER (gray rectangle) is composed of a tRNA-like gene (red triangle) linked to one or two pre-miRNA stem-loops (light and dark blue rectangles). Proposed naming of all putative MHV68 miRNAs, which incorporates current miRBase number designations, is indicated. (Inset) Mfold *in silico* prediction of TMER1 structure and corresponding miRNA locations.

sets (see Table S2 in the supplemental material) designed to detect 17 confirmed or putative mature MHV68 miRNAs. As detailed in Table S1 in the supplemental material, these sequences included the previously confirmed miRNA sequences: mghv-miR-M1-1-3p and mghv-miR-M1-10-5p (TMER1), mghv-miR-M1-3-3p (TMER2), mghv-miR-M1-4-5p (TMER3), mghv-miR-M1-5-5p, mghv-miR-M1-6-3p (TMER4), mghv-miR-M1-7-5p and mghv-miR-M1-7-3p (TMER5), mghv-miR-M1-13-5p (TMER6), mghv-miR-M1-14-3p (TMER7), and mghv-miR-M1-15-5p and mghv-miR-M1-9-3p (TMER8). Sequences of several putative miRNAs were also included in the study: mghv-miR-M1-2-5p (TMER2), mghv-miR-M1-8-5p, mghv-miR-M1-8-3p and mghv-miR-M1-13-3p (TMER6), and mghv-miR-M1-15-3p (TMER8).

To provide a framework for examining the presence of MHV68 miRNAs during latent infection *in vivo*, we first confirmed miRNA expression in cells lytically or latently infected *in vitro*. For assessment of expression during acute replication, NIH 3T12 fibroblasts were infected with wild-type MHV68 at a multiplicity of infection (MOI) of 5, and cells were harvested at 0, 6, 16, 24, and 48 h postinfection (hpi). RNA was then subjected to stem-loop qRT-PCR. To control for experimental variability, primers and probe sets specific for cellular small nucleolar RNA (snoRNA) 234 or snoRNA202 (see Table S2 in the supplemental material) were included in all experiments, as these small noncoding RNAs are generally stable during MHV68 infection (see Fig. S1). A standard curve using synthetic mghv-miR-M1-2-5p (miRIDIAN) (see Fig. S2) was also used to determine the approximate copy number per cell of each miRNA. Results from these experiments, expressed as values relative to those for snoRNA234 (Fig. 2A) or as relative numbers of copies per cell (Fig. 2B), demonstrated time-dependent and differential expression of MHV68 miRNAs. During the entire time course, 7 of the 17 mature miRNAs were induced to high levels, including 5 that were expressed at >1,000 copies per infected cell. In general terms, expression of the 7 highest-level miRNAs was detectable in two waves within the 48 h, with peak expression for 5 miRNAs (mghv-miR-M1-2-5p, mghv-miR-M1-3-3p, mghv-miR-M1-8-5p, mghv-miR-M1-13-5p, and mghv-miR-M1-15-5p) occurring at 16 or 24 hpi (Fig. 2C) and peak expression of the other 2 (mghv-miR-M1-5-5p and mghv-miR-M1-15-3) at 48 hpi (Fig. 2D). Interestingly, the prospective miRNAs mghv-miR-M1-15-3p, mghv-miR-M1-2-5p, and mghv-miR-M1-8-5p were detected above 1,000 copies/cell at 16 to

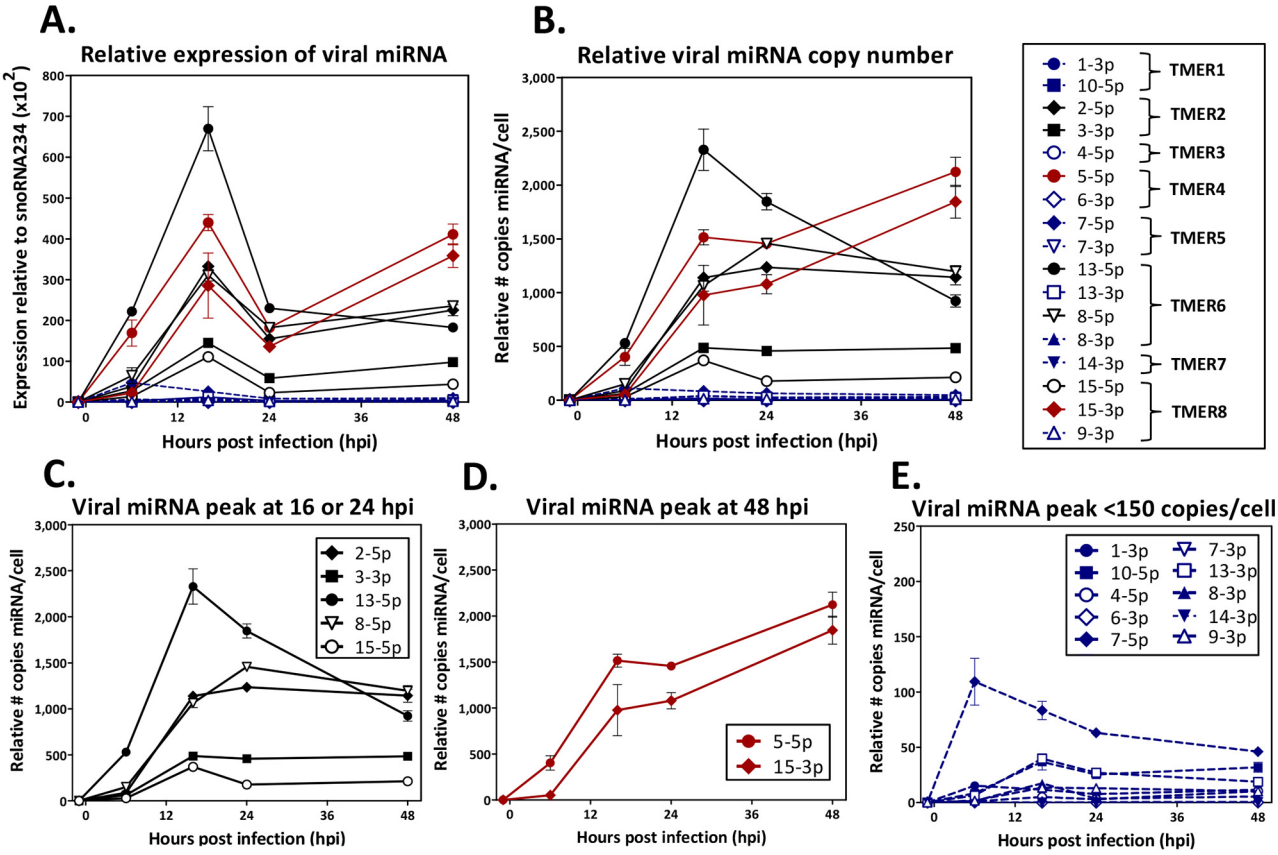

FIG 2 Expression kinetics of MHV68-encoded miRNAs during lytic infection. Stem-loop qRT-PCR was used to determine the level of expression of MHV68-encoded mature miRNAs during lytic replication. NIH 3T12 fibroblasts were infected with MHV68 at MOI 5 and then harvested at the indicated time points. Stem-loop qRT-PCR was performed using TaqMan primers and probe sets (see Table S2 in the supplemental material). (A) Expression time course for all tested viral miRNAs relative (10^2) to the endogenous noncoding RNA control snoRNA234. (B) Time course for all tested viral miRNAs expressed as approximate miRNA copy number per cell, based on the synthetic miR-2-5p standard curve. (C) Viral miRNAs that peak between 16 and 48 hpi, expressed as miRNA copy number per cell. (D) Viral miRNAs that peak at 48 hpi. (E) Viral miRNAs with consistent low-level expression throughout the time course, depicted on an enhanced scale. All data are means ± standard deviations (SD) from 3 experiments.

24 hpi or after 48 h, strongly suggesting that these represent legitimate mature miRNAs. The 10 other miRNAs tested were expressed at levels below 150 copies/cell (Fig. 2E). Although some of these miRNAs appeared to be slightly induced during infection, only mghv-miR-M1-7-5p was detected above 50 copies per cell. Together these data demonstrated that the expression of both previously annotated and prospective MHV68 miRNAs varied widely and could be subdivided into at least 3 kinetic classes. Because these miRNAs utilize similar polymerase III promoter sequences, these results strongly suggest that additional posttranscriptional mechanisms regulate MHV68 miRNA expression, such as processing efficiency and/or stability.

To determine whether the profile of MHV68 miRNA expression differed during latency compared to lytic replication, we performed identical stem-loop qRT-PCR assays using two latently infected B cell lines (Fig. 3A): S11, a naturally infected B cell line subcultured from BALB/c splenic lymphoma (45), and HE2.1, a line that was generated by antibiotic selection of A20 murine B cells infected with a recombinant MHV68 carrying a hygromycin resistance cassette (46). To obtain steady-state expression levels during latency, S11 and HE2.1 cells were lysed during stable growth *in vitro*. Although several of the miRNAs expressed during lytic replication in fibroblasts were also detected in latently infected B cells, the overall miRNA expression profiles differed. Most notably, one of the two miRNAs most abundantly expressed during lytic replication, mghv-miR-M1-15-3p, was nearly undetectable in S11 and HE2.1 B cells. In contrast, mghv-miR-M1-1-3p was expressed in both latently infected cell lines but was not readily detected in lytically infected fibroblasts. In contrast to these clear differences, at least two MHV68-encoded miRNAs, mghv-miR-M1-2-5p and mghv-miR-M1-5-5p, were expressed at high levels during both lytic replication and latency. In general terms, viral miRNA expression was significantly lower in latently infected cell lines than in lytically infected cells; for example, at peak levels in NIH 3T12 cells, the expression of mghv-miR-M1-5-5p was 700-fold and 189-fold higher than expression in S11 and HE2.1 cells, respectively. Although S11 and HE2.1 B cells displayed similar profiles of viral miRNAs expressed, the level of expression was higher in HE2.1 than S11 cells (e.g., mghv-miR-M1-2-5p, -3-3p, and -5-5p levels were, respectively, 8.4-fold, 5.3-fold, and 3.8-fold higher in HE2.1 cells). In addition, mghv-miR-M1-8-5p and mghv-miR-M1-9-3p were detectable in HE2.1 cells but not S11 cells, indicating that MHV68-encoded miRNA expression is at least partially cell line dependent.

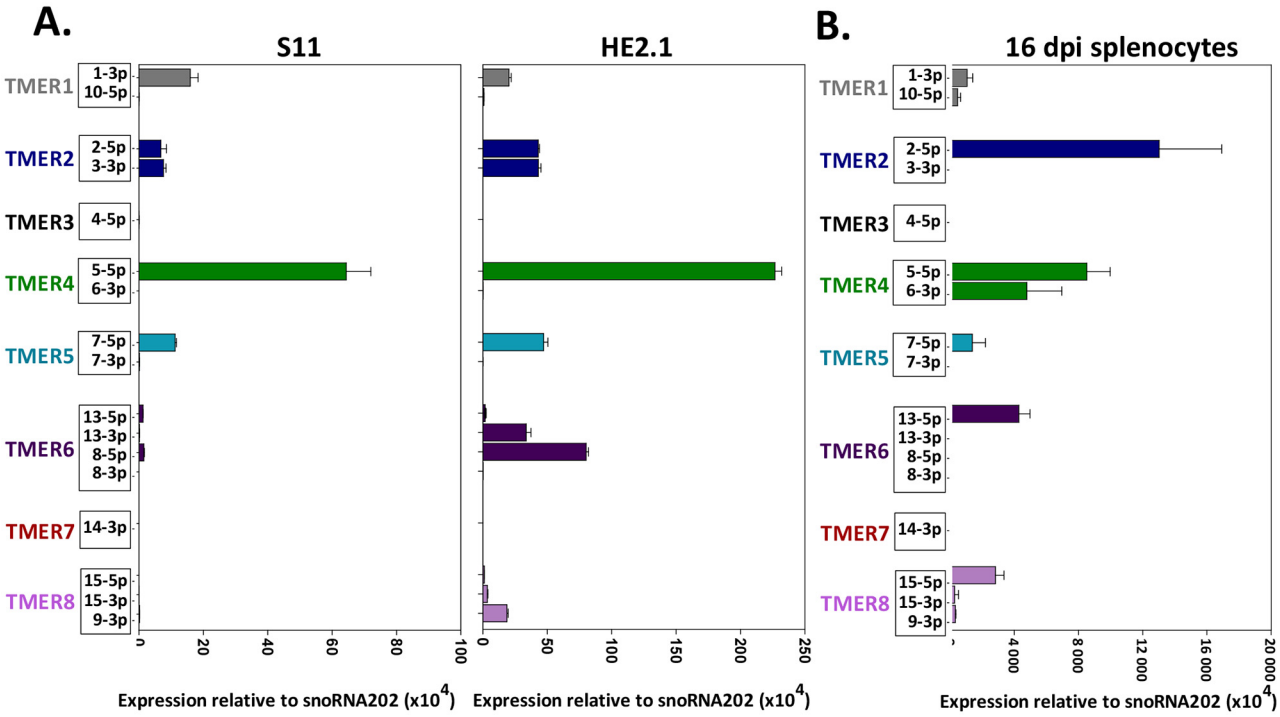

FIG 3 Expression of MHV68-encoded miRNAs during latent infection. Stem-loop qRT-PCR was used to determine the level of expression of MHV68-encoded mature miRNAs during latent infection *in vitro* and *in vivo*. (A) miRNA expression from S11 and HE2.1 B cell lines with stable latent MHV68. Following cell harvest and lysis, stem-loop qRT-PCR was performed using TaqMan primers and probe-sets (see Table S2 in the supplemental material). Displayed values are relative (10^4) to endogenous snoRNA202 expression. Values are means ± SD from 3 experiments. (B) miRNA expression from splenocytes latently infected *in vivo*. For each experiment, four C57BL6/J mice were infected i.n. with 10^4 PFU MHV68. At 16 days, splenocytes were harvested and pooled, lysed, and subjected to stem-loop qRT-PCR. Values are relative (10^4) to endogenous snoRNA202 expression and are means ± SD from 2 experiments.

In order to define whether the profile of MHV68-encoded miRNAs expressed during latent infection *in vivo* was similar to that observed in latently infected B cell lines, we performed stem-loop qRT-PCR assays on splenocytes harvested from mice latently infected with MHV68 (Fig. 3B). For these experiments, wild-type C57BL/6J (B6) mice were inoculated intranasally (i.n.) with 10^4 PFU MHV68, and splenocytes were harvested at 16 days post-inoculation, a time point at which acute replication is no longer detectable and latent infection is maximal (1 infected cell per 100 to 200 splenocytes) (47, 48). Interestingly, the *in vivo* viral miRNA expression profile differed both qualitatively and quantitatively from the profiles of S11 and HE2.1 B cell lines. For example, while the expression of mghv-miR-M1-3-3p and mghv-miR-M1-8-5p was observed in both lytically and latently infected cell lines, neither miRNA was detected in *in vivo* samples. Conversely, mghv-miR-M1-6-3p and mghv-miR-M1-15-5p were detected at high levels in splenocytes from infected mice but were nearly undetectable in cell lines. In fact, the miRNA encoded on the opposing strand, mghv-miR-M1-15-3p, was one of the two most highly expressed miRNAs in lytically infected cells. Thus, splenocytes at 16 dpi displayed a miRNA expression profile distinct from that of cells infected *in vitro*. Together, these results demonstrate that the expression of MHV68 miRNAs is tightly regulated and is likely dependent upon both the phase of virus life cycle and the cell type infected.

Generation of an MHV68 mutant virus deficient in miRNA expression. To determine the role of the virus-encoded miRNAs in MHV68 replication, latency, and pathogenesis, we generated a recombinant virus carrying 13 separate mutations that deleted or blocked expression of all 14 pre-miRNA stem-loops (Fig. 4A; also, see Table S1 in the supplemental material). The miRNA mutant virus, MHV68.Zt6, was generated by two-step lambda Red-mediated recombination (49) using three separate molecular constructs. To facilitate the detection of virus-infected cells *in vivo*, MHV68.Zt6 was created on the backbone of the MHV68.ORF73βla marker virus, which we described previously (47, 50). For miRNAs encoded by TMER1 to TMER5, TMER7, and TMER8, pre-miRNA stem-loop sequences were conservatively deleted, leaving intact the tRNA promoter, vtRNA sequence, and tRNA stop sequence and all intervening vtRNA-to-pre-miRNA and pre-miRNA-to-pre-miRNA sequences. For all mutations, the modified TMER sequences were analyzed *in silico* using the mfold RNA folding tool (51) to ensure that the predicted vtRNA structure was not affected. Because the mghv-miR-M1-13 and mghv-miR-M1-8 stem-loops (encoded by TMER6) are located within the 3′ UTR of the important MHV68 latency gene M2 (52, 53), we opted to insert a polymerase III (PolIII) stop sequence upstream of the pre-miRNAs as an alternative to deleting the sequences. A string of six deoxythymidine (T) nucleotides was inserted after vtRNA6 (Fig. 4A; also, see Table S1 in the supplemental material). Following cloning and recombination, the resulting mutant virus bacterial artificial chromosome (BAC) clones were carefully screened using pulsed-field gel electrophoresis (PFGE) and Sanger sequencing of the mutated region. A single clone was then selected for whole-genome high-throughput sequencing (see Fig. S3 in the supplemental material). Impor-

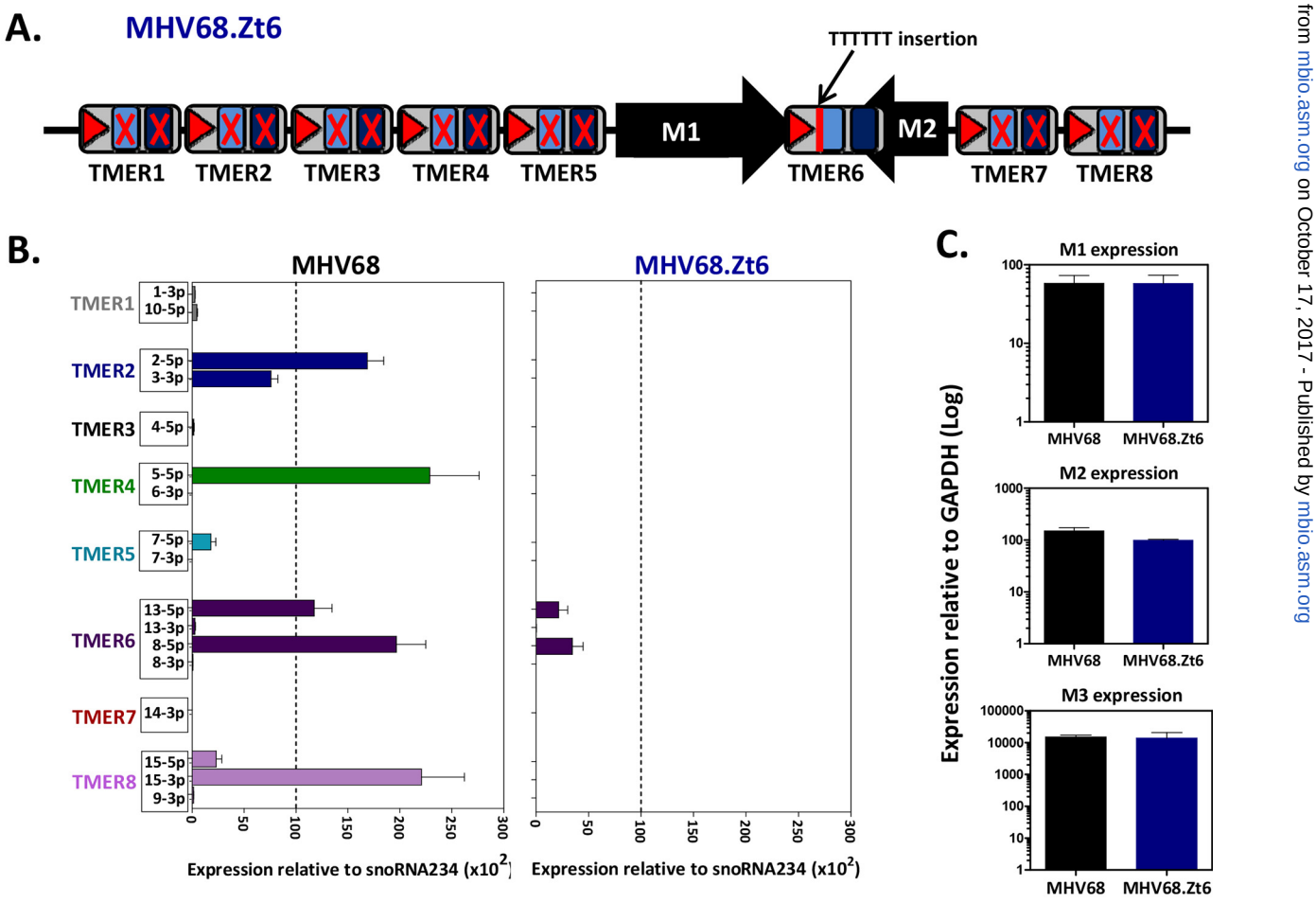

FIG 4 miRNA mutations incorporated in MHV68.Zt6 and corresponding expression of miRNAs and surrounding genes. (A) Depiction of MHV68.Zt6 mutations, including deletion of TMER1 to TMER5, TMER7, and TMER8 miRNA stem-loops (red X) and insertion of the PolIII stop site (red line) following vtRNA6 in TMER6. (B) Expression of viral miRNAs from wild-type MHV68 marker virus or MHV68.Zt6, relative (10^2) to the endogenous noncoding RNA control snoRNA202. NIH 3T12 fibroblasts were infected with MHV68.ORF73βla or MHV68.Zt6 at an MOI of 5 and then harvested at 48 hpi. Stem-loop qRT-PCR was performed as described for >Fig. 1. Values are means ± SD from 2 experiments. (C) Expression of viral coding genes surrounding miRNA mutations. NIH 3T12 fibroblasts were infected with MHV68.ORF73βla or MHV68.Zt6 at an MOI of 5 for 24 h. M1, M2, and M3 expression was quantified using qRT-PCR. Values are relative (10^3) to endogenous GAPDH expression and are means ± SD from 3 experiments.

tantly, the MHV68.Zt6 genome carried all of the anticipated mutations but did not harbor any unintended secondary mutations and was otherwise identical to the parental MHV68.ORF73βla genome.

To confirm whether the MHV68.Zt6 mutations eliminated miRNA expression, we infected NIH 3T12 fibroblasts with MHV68 or MHV68.Zt6 and performed stem-loop qRT-PCR on samples harvested at 48 h (Fig. 4B). As expected, miRNAs encoded by TMER1 to TMER5, TMER7, and TMER8 were not detected. While the expression of mghv-miR-M1-13-5p and mghv-miR-M1-8-5p in cells infected with MHV68.Zt6 was reduced 82% compared to that in cells infected with wild-type MHV68, both mature miRNAs were still detectable at levels above background (Fig. 4B; also, see Fig. S4 in the supplemental material), indicating that insertion of the PolIII stop sequence downstream of vtRNA6 significantly reduced but did not completely eliminate the expression of TMER6-encoded miRNAs. Notably, none of the TMER mutations resulted in loss of vtRNA stability, as all eight vtRNAs were readily detected in infected cells (data not shown).

Because the miRNA mutations in MHV68.Zt6 were inserted in the genomic region proximal to the protein-coding genes M1, M2, and M3, we verified the expression of these genes using qRT-PCR (Fig. 4C). NIH 3T12 fibroblasts were infected with MHV68.ORF73βla or MHV68.Zt6, and qRT-PCR was performed on samples harvested at 24 h. MHV68.Zt6-infected cells expressed M1, M2, and M3 at levels nearly equivalent to those in wild-type MHV68-infected cells, demonstrating that insertion of the 13 miRNA mutations had no significant effect on expression of surrounding protein-coding genes.

MHV68 miRNAs are dispensable for lytic virus replication. To determine whether the MHV68-encoded miRNAs played a role in lytic replication, we quantified replication of the total miRNA mutant virus versus the parental wild-type MHV68.ORF73βla virus in both *in vitro* and *in vivo* assays. For *in vitro* single-step and multistep growth curves, NIH 3T12 fibroblasts were infected with each virus at MOI of 5 and 0.5, respectively. Samples were harvested at intervals from 0 to 48 h for single-step curves and 0 to 120 h for multistep curves, and virus

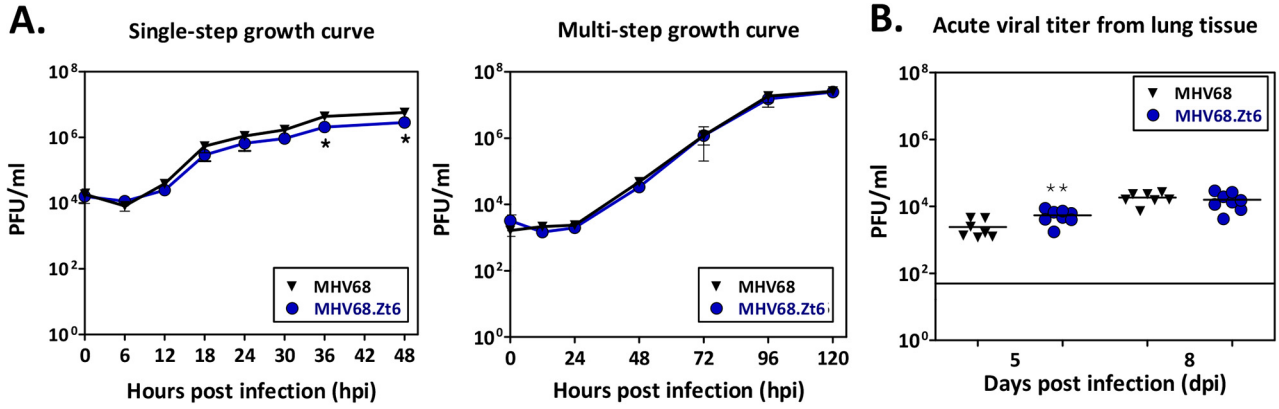

FIG 5 MHV68 miRNAs are dispensable for lytic replication. Plaque assays were used to determine the titer of wild-type or miRNA deletion mutant viruses during acute replication *in vitro* and *in vivo*. (A) Lytic replication in fibroblasts *in vitro*. Single-step and multistep growth curves were generated following infection of NIH 3T12 fibroblasts with MHV68.ORF73βla or MHV68.Zt6 at an MOI of 5 or 0.05, respectively. At the specified time points, cells and supernatant fluid were collected, and titers were determined by plaque assay. Data are means ± SD of 3 experiments. (B) Lytic replication in lungs *in vivo*. C57BL6/J mice were infected i.n. with 10^4 PFU MHV68.ORF73βla or MHV68.Zt6. At 5 or 8 dpi, lungs were harvested and viral titers were determined by plaque assay. Lines represent the mean titers for eight individual mice. For all experiments, statistical significance was determined by Student's *t* test. *, $P < 0.05$; **, $P < 0.01$.

titers were determined by plaque assay (Fig. 5A). Although in single-step growth curves MHV68.Zt6 appeared to replicate at slightly lower levels than wild-type virus at late time points, replication of the mutant virus was identical to that of wild-type virus in multistep growth curves, indicating that any defect in MHV68.Zt6 growth is minimal. To determine whether lytic replication of the mutant virus was compromised *in vivo*, we infected wild-type B6 mice i.n. with 10^4 PFU MHV68.ORF73βla or MHV68.Zt6 and then performed plaque assays on lungs harvested at 5 and 8 days postinoculation (Fig. 5B). Surprisingly, MHV68.Zt6 replicated to slightly higher titers than wild-type virus at 5 dpi; however, this difference disappeared by 8 dpi, indicating that any replication differences are relatively minor. Thus, together these results demonstrate that the MHV68-encoded miRNAs are dispensable for lytic virus replication in the lung.

Virus-encoded miRNAs modulate MHV68 latency and reactivation. To determine the role of MHV68-encoded miRNAs in chronic infection, we performed a series of *in vivo* assays to evaluate the ability of MHV68.Zt6 to establish and reactivate from latency. Wild-type B6 mice were infected i.n. with 10^4 PFU (Fig. 6A) or 100 PFU (Fig. 6B) of wild-type virus (parental MHV68.ORF73βla) or total miRNA mutant virus (MHV68.Zt6). Sixteen (10^4 PFU) or nineteen (100 PFU) days later, after the clearance of acute replication, spleens were harvested and pooled from four mice per sample group (per experiment, $n = 7$ for 10,000 PFU and $n = 4$ for 100 PFU). For each experiment, pooled single-cell splenocyte suspensions were subjected to parallel assays to detect the presence of viral genome, the presence of preformed infectious virus, and the ability of infected cells to spontaneously reactivate from latency. Limiting-dilution nested-PCR assays (47, 54), which can detect a single copy of viral genome in a background of 10,000 uninfected cells, were used to determine the frequency of splenocytes that harbored viral genome (Fig. 6A, left). Consistent with our previous results (47), infection with wild-type MHV68.ORF73βla virus resulted in the establishment of infection in approximately 1 in 260 splenocytes. In contrast, mutation of the virus-encoded miRNAs resulted in a 2.3-fold reduction, to a frequency of 1 in 600. Although this represented a relatively small change from wild-type virus infection, these results were statistically significant and highly reproducible over 7 independent experiments. Furthermore, a similar reproducible reduction in MHV68.Zt6 infection was observed following 100 PFU inoculations (Fig. 6B, left).

To determine whether MHV68.Zt6-infected cells exhibited an altered ability to reactivate from latency, parallel splenocyte samples were plated in limiting dilutions on mouse embryonic fibroblast (MEF) monolayers. Spontaneous *ex vivo* reactivation events were determined by observation of cytopathic effect (CPE) on MEF monolayers. Surprisingly, despite the reduction in cells infected with MHV68.Zt6, the frequency of reactivation was nearly identical to that of wild-type virus when both were administered at 10^4 PFU (Fig. 6A, middle) (1 in 23,000 for MHV68.ORF73βla; 1 in 27,500 for MHV68.Zt6). In contrast, though, when both viruses were given at 100 PFU (Fig. 6B, middle), reactivation of MHV68.Zt6-infected cells (1 in 100,500) was reduced 4.4-fold compared to that of cells infected with wild-type virus (1 in 23,000). To ensure that infected cells were not undergoing lytic replication at the time of harvest, parallel splenocyte samples were mechanically disrupted, which destroys cells but does not damage virus particles (48), and then plated in limiting dilution on fibroblast monolayers (Fig. 6, right panels). As expected, CPE on MEF monolayers was not reproducibly observed in samples from any infection group, indicating that infected splenocytes lacked preformed infectious virus and confirming that these cells were latently infected. Together, these results demonstrate that the MHV68-encoded miRNAs modulate processes involved in the normal establishment of virus latency and reactivation and that their effects may be in part dose dependent, as has been observed for the critical latency gene M2 (52).

MHV68-encoded miRNAs modulate infection of germinal-center and memory B cells. MHV68 infects multiple mature B cell subsets, including naive, germinal-center, and memory B cells. To determine whether the splenic latency attenuation observed in viral genome PCR assays was due to reduced infection of one or more specific B cell subsets, we performed multiparametric flow cytometric analyses of cells expressing the virus-encoded beta-

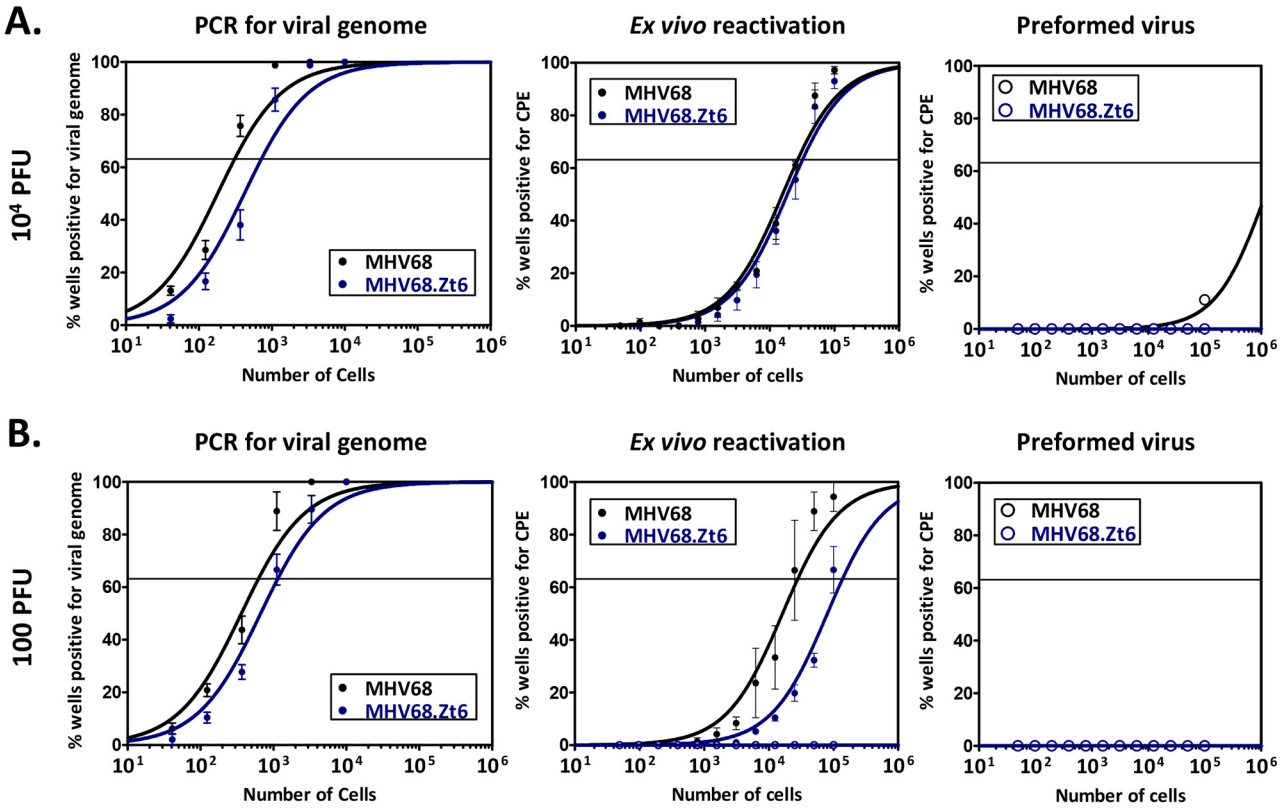

FIG 6 MHV68 miRNAs modulate latency and reactivation *in vivo*. Parameters of wild-type and miRNA mutant virus latency and reactivation were assessed 16 to 19 dpi. For each experiment, four C57BL6/J mice were infected i.n. with MHV68.ORF73βla or MHV68.Zt6 at (A) 10^4 PFU ($n = 7$ experiments) or (B) 100 PFU ($n = 4$ experiments). Sixteen (10^4 PFU) or nineteen (100 PFU) days later, splenocytes from each mouse were harvested, pooled within groups, and then subjected to limiting dilution assays to detect the presence of viral genome, *ex vivo* reactivation from latency, or the presence of preformed infectious virus. For viral genome assays, splenocytes were serially diluted 3-fold in a background of uninfected cells, plated at 12 reactions per cell dilution, lysed, and then subjected to nested PCR specific for MHV68 ORF72. This assay is specific for a single copy of viral genome in a background of 10,000 uninfected cells. The frequency of cells harboring viral DNA was determined using a Poisson distribution, indicated by the line at 63.2%. For reactivation assays, splenocytes were serially diluted 2-fold and then plated at 24 wells per cell dilution over a monolayer of mouse embryonic fibroblasts (MEFs). After 3 weeks, monolayers were assessed for cytopathic effect (CPE) following spontaneous reactivation from latency. To detect preformed infectious virus, parallel cell samples were mechanically disrupted prior to plating on MEF monolayers. The frequencies of splenocytes reactivating from latency or carrying preformed virus was determined using a Poisson distribution, as indicated by the line at 63.2% ($n = 3$ experiments).

lactamase marker. The miRNA mutant virus MHV68.Zt6 and its parental wild-type counterpart MHV68.ORF73βla incorporate a modified beta-lactamase as a C-terminal fusion to the latency-associated nuclear antigen (mLANA) (47). mLANA is critical for the maintenance of the viral episome during latency and is therefore expressed in a large fraction of latently infected B cells, including developing, naive, germinal-center, and memory B cells (47, 50). Virus-infected cells expressing mLANA-β-lactamase (mLANA-βlac) fusion protein are detectable following staining with CCF4/AM (Life Technologies), a fluorogenic beta-lactamase substrate whose emission wavelength is altered when cleaved. For experiments described here, four B6 mice per sample group per experiment were infected with 10^4 or 100 PFU of virus, and then splenocytes were harvested at 16 or 19 days, respectively. To detect infected B cell subsets, splenocytes from each sample group were pooled and then stained with CCF4/AM and a combination of antibodies directed toward appropriate B cell surface markers, including CD19, IgM, and CD38 or PNA (peanut agglutinin). In all experiments, 0.096 to 0.295% of the cells were positive for mLANA-βlac (Fig. 7A and data not shown). In most experiments, gated mLANA-βlac$^+$ cells were identified as naive B cells (CD19$^+$ IgM$^+$), germinal-center B cells (CD19$^+$ IgM$^-$ CD38$^{-/lo}$ or CD19$^+$ IgM$^-$ PNA^{hi}) or memory B cells (CD19$^+$ IgM$^-$ CD38^{hi} or CD19$^+$ IgM$^-$ PNA$^{-/lo}$), as previously described (7, 47, 55, 56).

Interestingly, regardless of infectious dose, the miRNA mutant virus MHV68.Zt6 consistently displayed an altered distribution of infected B cells (Fig. 7B and C), with an overall increase in infected naive and/or germinal-center B cells and a partially compensatory reduction in memory B cells. For example, in mice inoculated with 10^4 PFU MHV68.Zt6, the fraction of mLANA-βlac$^+$ cells that were naive B cells increased by 13.0% (from 62.7 to 70.9), and the fraction that were germinal-center B cells increased by 45.8% (from 10.8 to 15.8). In contrast, the fraction that were memory B cells decreased by 48.8% (from 12.3 to 6.3). Similarly, following 100-PFU inoculation, naive B cells increased by 20.9%, while memory B cells decreased by 22.8%. The recovery of germinal-center B cells from this low-dose inoculation was inconsistent and not statistically significant in either direction. Cumulatively, these results demonstrate that the virus-encoded miRNAs alter the distribution of B cells infected with MHV68 and may play a particularly important role in facilitating the entry of infected B cells into the memory B cell reservoir.

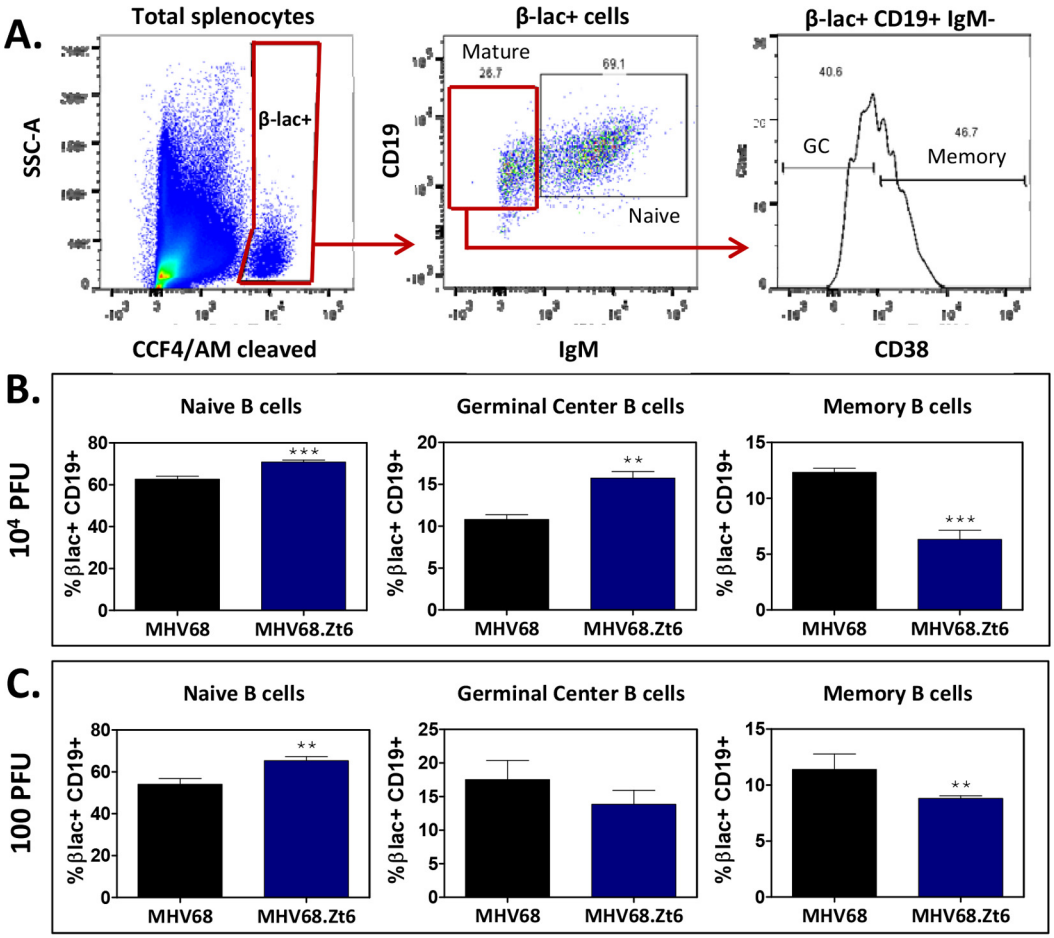

FIG 7 MHV68 miRNAs contribute to efficient infection of memory B cells *in vivo*. Flow-cytometric detection of β-lactamase activity and cell surface marker costaining were used to determine the phenotype of B cells infected *in vivo*. Three C57BL6/J mice per sample group per experiment were infected i.n. with parental wild-type MHV68.ORF73βla, or miRNA mutant MHV68.Zt6. After 16 days, splenocytes were harvested, pooled, and then stained with antibodies for CD19, IgM, and CD38, in addition to the β-lactamase substrate CCF4/AM. Single-cell suspensions were then subjected to flow-cytometric analyses. (A) Schematic of representative flow cytometry gating scheme to quantify the percentage of infected naive ($CD19^+$ IgM^+), germinal-center ($CD19^+$ IgM^- $CD38^{lo}$) and memory ($CD19^+$ IgM^- $CD38^{hi}$) B cells. (B and C) Mice were infected i.n. with 10^4 (4 experiments) or 100 (5 experiments) PFU of parental wild-type MHV68.ORF73βla or the miRNA mutant MHV68.Zt6. Values are percentages of infected $CD19^+$ cells from each sample group displaying a naive, germinal-center, or memory B cell surface marker phenotype. Statistical significance was determined using Student's *t* test. **, $P < 0.01$; ***, $P < 0.005$.

MHV68-encoded miRNAs are required for lethal viral pneumonia in IFN-γ-deficient mice. Given the phenotype of MHV68.Zt6 in latency and reactivation assays, we sought to further scrutinize the role of MHV68-encoded miRNAs during gammaherpesvirus disease. Gamma interferon (IFN-γ) is an important enhancer of host immunity that has been shown to play key roles in the regulation of several viruses, including MHV68 (32, 57). For example, although IFN-γ-deficient mice clear acute MHV68 replication normally, latently infected cells from these mice display increased reactivation and persistent replication (58, 59). This loss of control of chronic infection correlates with a high degree of susceptibility to vascular and pulmonary inflammatory diseases, including large-vessel vasculitis (60), pulmonary fibrosis (61), pulmonary B cell lymphoproliferative disease (62), pulmonary lymphoma (62), and lethal, virus-associated pneumonia (63).

To determine whether miRNAs encoded by MHV68 facilitate virus-associated disease, we tested the miRNA deletion mutant MHV68.Zt6 for the ability to induce pulmonary inflammation and pneumonia. For these experiments, 9 to 16 BALB/c.IFN$\gamma^{-/-}$ mice per group were inoculated i.n. with 4×10^5 PFU of MHV68, MHV68.ORF73βla, or MHV68.Zt6, and infection was allowed to progress for up to 14 days. As expected, ≥75% of mice infected with wild-type strains MHV68 (7 of 9) and MHV68.ORF73βla (12 of 16) succumbed to lethal pneumonia within the 14-day time course (Fig. 8). However, in stark contrast, 0 of 15 MHV68.Zt6-infected mice died. This outcome correlated with the magnitude of inflammatory pulmonary infiltrates, as wild-type-virus-infected mice that succumbed to disease displayed >80% involvement in lung tissue with a predominance of cellular infiltrates (Fig. 9). In contrast, mice infected with the miRNA mutant virus displayed only mild signs of interstitial and perivascular mononuclear infiltrates. Interestingly, the strong attenuation displayed by MHV68.Zt6 parallels results previously noted for MHV68 cyclin D and Bcl-2 ortholog mutant viruses (63)—mutants that, like MHV68.Zt6, undergo normal acute replication but have a defect in reactivation from latency. Thus, the data presented here demonstrate that the MHV68-encoded miRNAs are required for the

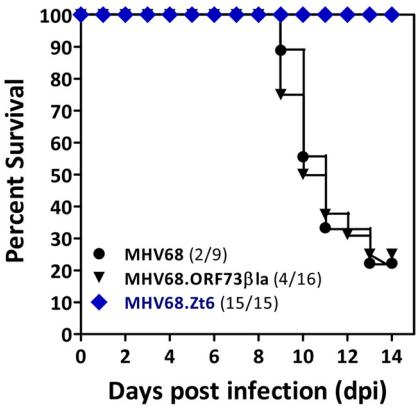

FIG 8 MHV68 miRNAs are essential for lethal pneumonia. Survival of IFN-γ-deficient mice from MHV68-associated lethal pneumonia during a 14-day infection time course is shown. BALB/c.IFN$\gamma^{-/-}$ mice were infected i.n. with 4×10^5 PFU of MHV68, MHV68.ORF73βla, or MHV68.Zt6 and monitored daily for signs of disease. Data are the percentage of mice surviving infection at each time. Parenthetical values are the numbers of mice surviving 14 dpi/number of mice tested.

development of virus-induced pulmonary inflammation and lethal pneumonia and further substantiate the link between viral genes that facilitate control of latency and reactivation and those that cause disease in mice deficient in IFN-γ function.

DISCUSSION

Following the seminal report by Pfeffer and colleagues identifying EBV-encoded miRNAs (10), the study of viral miRNAs has expanded remarkably, particularly in the herpesvirus field. Advances in high-throughput sequencing and CLIP technology, along with the development of computational algorithms for miRNA target predictions, have led to the identification of numerous herpesvirus miRNA targets (14, 16). However, to date, few studies have examined the functions of these miRNAs in natural host-virus infection systems. Here, we present evidence of the expression and *in vivo* roles of gammaherpesvirus miRNAs in the context of natural infection. Utilizing a recombinant virus that exhibits eliminated or reduced expression of miRNAs from all 14 known pre-miRNA stem-loops, we demonstrate that while the MHV68-encoded miRNAs are largely dispensable for acute replication, the total miRNA mutant virus is partially attenuated for latency and reactivation *in vivo*. Examining specific B cell subsets that harbor the mutant virus revealed a specific loss of infection in the memory B cell compartment. Interestingly, this reduction correlated with a reciprocal increase in infection of naive follicular and germinal-center B cells, perhaps reflecting a block in the differentiation of infected cells into the memory compartment. Most notably, virus-encoded miRNAs were essential for lethal pneumonia. Together, these findings reveal a role for virus-encoded miRNAs in MHV68 latency and pathogenesis.

MHV68 miRNA expression. We have quantified the expression of a defined set of previously confirmed and predicted mature miRNAs. Using a stem-loop PCR approach, we demonstrated that the pattern of MHV68-encoded miRNA expression is dependent on both the stage of infection and the cell type infected. For example, although 5 of the 6 miRNAs detected at high levels during lytic fibroblast infection were also observed in at least one latent-infection cell type (S11 B cells, HE2.1 B cells, or splenocytes), mghv-miR-M1-15-3p was detected at appreciable levels only during lytic replication. In contrast, mghv-miR-M1-6-3p and mghv-miR-M1-15-5p were detected only in latently infected cells harvested from *in vivo* samples. While miRNA expression was highly reproducible among biological replicates, and at least one miRNA—mghv-miR-M1-5-5p—was consistently detected at higher levels than others across different cell types and conditions, the findings presented here demonstrate the significant variability in expression of MHV68-encoded miRNAs among experimental conditions. Additionally, these data make it clear that cell lines are not necessarily valid models with which to identify miRNAs that are expressed under biologically relevant conditions *in vivo*.

The disparate miRNA expression profiles among cell types tested here likely reflect several variables. Because the transcription of the eight MHV68 TMERs is driven by similar PolIII promoters, the detection of various levels of mature miRNAs likely

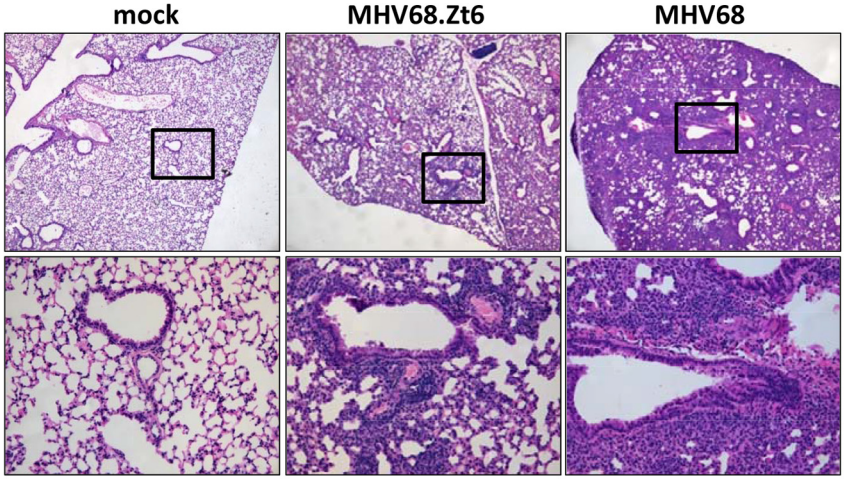

FIG 9 MHV68.Zt6 displays reduced lung inflammation in IFN-$\gamma^{-/-}$ mice. Hematoxylin and eosin (H&E) stains of lung sections from infected mice are shown. Following harvest, lungs from infected mice were fixed, embedded in paraffin, sectioned, and stained with H&E. (Top) Magnification, ×10. (Bottom) Higher (×40) magnifications of boxed portions in top row.

involves differential processing of the TMER primary RNA (pri-miRNA) transcripts and/or pre-miRNA stem-loops. This conclusion would be consistent with the existence of additional regulatory pathways for controlling cell type-specific maturation of viral and host miRNAs (64, 65). In support of this, in many cases, mature miRNAs from the same TMER transcript were detected at dissimilar levels in parallel samples. Cell-specific differences in the presence of individual mature miRNAs also likely reflect the particular transcriptome, as the stability of individual mature miRNAs is strongly influenced by the presence of cognate target transcripts and subsequent protection by RISC Argonaute proteins (66, 67). Finally, it is important to note that stem-loop primers are highly sensitive to sequence specificity and are unable to efficiently prime cDNA synthesis from alternate mature miRNA sequences. Thus, the TaqMan assays utilized here do not detect all alternate miRNA isoforms that may be present in some cell types at a higher abundance than the published sequence (68).

MHV68 miRNAs are dispensable for acute replication. We found that the MHV68 miRNAs are largely dispensable for acute replication in fibroblasts *in vitro* and in lungs *in vivo*. These findings are in accordance with previous reports that demonstrated that spontaneous MHV68 mutants missing the leftmost ~9.5 kb of the genome (which includes TMER1 through TMER8, M1, M2, and M3) display normal acute replication (69, 70). The observation that mutation of the viral miRNAs has no phenotypic consequence for acute replication is completely consistent with the expected subtle roles of miRNAs in regulating transcription, particularly in the context of the high levels of lytic transcripts (71). However, this conclusion does not imply that the MHV68-encoded miRNAs play no role in regulating transcripts associated with lytic replication; indeed, it is likely that at least some herpesvirus miRNAs serve to regulate "leaky" lytic transcripts in cells in which the virus operates a latency transcription program (13, 71). Notably, though, an MHV68 mutant that is mutated in the PolIII promoters of all 8 TMERs, and thus lacks expression of both vtRNAs and miRNAs, is slightly delayed in lytic replication (Diebel et al., submitted). Thus, together these results may suggest that the vtRNAs themselves play an unforeseen role in acute MHV68 replication.

Are MHV68 miRNAs critical for transition to latency in the memory B cell compartment? The biological mechanisms that govern the *in vivo* establishment and maintenance of lifelong gammaherpesvirus latency remain incompletely understood. Work from numerous laboratories studying EBV and MHV68 latency has led to the widely accepted virus-driven B cell maturation model, in which the virus infects naive B cells and, independent of cognate B cell receptor antigen, guides their differentiation to memory B cells (72). Results presented here clearly demonstrate a role for the virus-encoded miRNAs in modulation of specific aspects of MHV68 latency. Mutation of MHV68 miRNAs resulted in a minor but reproducible defect in the frequency of bulk splenocytes that harbor the viral genome. This defect was not due to effects on the important latency gene M2, since M2 expression was normal in cells infected with the MHV68.Zt6 mutant and this phenotype is substantially less pronounced than that previously observed for M2 and left-end deletion mutants of MHV68 (52, 69, 70, 73). The effect of miRNA mutation on reactivation efficiency in bulk splenocytes was generally unclear, as changes in reactivation were subtle and dependent upon dose. Interestingly, though, in-depth flow-cytometric analyses revealed that miRNA mutation led to a decrease in memory B cell infection. This reduction was accompanied by an accumulation of infected naive and germinal-center B cells. This reciprocal relationship is reminiscent of the accumulation of specific B cell subsets in genetically altered mice that are blocked in defined B cell development stages (for example, see reference 74), suggesting that the MHV68 miRNAs may contribute to B cell maturation. This conclusion is consistent with data obtained with KSHV demonstrating that miR-K12-11, a miR-155 ortholog, induces both murine and human B cell expansion *in vivo* during immune reconstitution (29, 30). Thus, while the *in vivo* maturation of infected naive B cells to memory B cells has not yet been directly demonstrated for MHV68, our results are consistent with a role for the MHV68 miRNAs in virus-driven maturation of B cells to the memory compartment. Alternatively, this phenotype may result from a reduced ability of the mutant virus to directly infect memory B cells.

MHV68 miRNAs are required for pathogenesis. At present it is not known whether virus-encoded miRNAs play any role in the pathogenesis of the various diseases associated with gammaherpesvirus infections. However, at least one alphaherpesvirus miRNA, Marek's disease virus mdv1-miR-M4, has been shown to be essential for the induction of T cell lymphomas in poultry (75). Consistent with a potential link for gammaherpesvirus-encoded miRNAs in disease, KSHV, EBV, and MHV68 miRNAs are detectable at high levels in virus-infected lesions and/or circulation from an array of lymphoproliferative disorders and tumors (42, 76–79), suggesting that these noncoding RNAs may play key pathogenic roles. Like the human viruses, MHV68 infection is associated with a high penetrance of disease in the setting of immunodeficiency, including lethal pneumonia, large-vessel vasculitis, lymphoproliferative disease, and B cell lymphoma. As an initial means to assess whether the MHV68 miRNAs contribute to pathogenesis, we tested the miRNA mutant virus in an established model of MHV68-induced pneumonia in which ~80% of virus-infected mice die within 14 days (63). Surprisingly, while mutation of the virus-encoded miRNAs had no effect on acute replication in the lung and only subtle effects on latency and reactivation in splenocytes, the absence of miRNA expression totally eliminated lethal pneumonia, demonstrating that the MHV68 miRNAs are essential for disease. Interestingly, these findings are consistent with the demonstration that a Marek's disease virus mutant lacking mdv1-miR-M4 displays normal acute replication and latency establishment but is highly attenuated for tumorigenesis (75). Together, these results may indicate that virus-encoded miRNAs are largely dispensable for normal infection but are central determinants of herpesvirus-associated disease.

The specific means by which the MHV68 miRNAs contribute to disease in this system are unknown, in large part because the biological mechanisms that lead to MHV68-associated pneumonia are poorly understood. Previous work has demonstrated that viruses that are highly attenuated in lethal pneumonia are deficient in either acute replication or reactivation from latency (63). However, MHV68.Zt6 demonstrated no defect in acute replication in lungs and a very subtle, dose-dependent defect in reactivation from latency in the spleen, suggesting that the MHV68 miRNAs mediate pathogenesis in this model by an alternative means. For example, it is possible that the MHV68 miRNAs directly contribute to the inflammatory response that underlies the development of disease. Such a finding would be consistent with the ability of some host miRNAs present in tumor cells to induce

prometastatic inflammatory responses (80). It is also conceivable that the virus-encoded miRNAs facilitate reactivation from a latency site not yet examined. MHV68 establishes latency in B cells and macrophages in the peritoneum (81) and in developing B cells in the bone marrow (50). Thus, it is possible that reactivation from one of these reservoirs is attenuated in the absence of miRNAs, although this would run counter to previous reports of herpesvirus-encoded miRNAs that suppress herpesvirus reactivation (82–85). It is possible that the pathogenic role of the MHV68-encoded miRNAs is opposed by the functions of IFN-γ, such that the true mechanistic basis of this pneumonia phenotype will only be revealed by further detailed analyses of infection in parameters in IFN-γ-deficient hosts. However, to date, we have observed only minor differences in acute replication in these animals (data not shown). Extensive work will be required to determine the viral mechanisms that underpin this striking attenuation.

Summary. The work presented here demonstrates for the first time an *in vivo* role for mammalian gammaherpesvirus miRNAs in latency and pathogenesis in the context of natural infection. Consistent with the anticipated limited molecular activity of these noncoding RNAs, our findings indicate that in the context of a normal course of infection, the MHV68 miRNAs likely serve as a rheostat to modulate specific biological outcomes. Using a combinatorial MHV68 mutant that is lacking miRNA expression from all 14 pre-miRNA stem-loops, we found that these miRNAs are dispensable for acute replication but play a role in the establishment of latency. Mutant virus infection was associated with a decrease in memory B cell infection and a reciprocal accumulation of infected naive and/or germinal-center B cells, perhaps implicating these miRNAs in virus-driven differentiation of infected B cells. However, extensive additional work will be required to define the specific mRNA targets of the biologically relevant miRNAs and to determine whether they are indeed critical for the maturation of infected B cells. Most notable from the work presented here, a lack of miRNA expression was associated with complete attenuation of lethal disease in a model of virus-induced pneumonia, indicating a central role for the MHV68 miRNAs in pathogenesis. Future work will be required to define which specific miRNAs mediate this key contribution and the precise role that they play in the genesis of disease.

MATERIALS AND METHODS

Cell lines and viruses. NIH 3T12 murine fibroblasts (ATCC CCL-164) and murine embryonic fibroblasts (MEFs) from C57BL/6J mice (Global Stem GSC-6002) were maintained in Dulbecco's modified Eagle's medium (DMEM) supplemented with 10% fetal calf serum, 100 U/ml of penicillin, 100 mg/ml streptomycin, and 2 mM L-glutamine. HE2.1 and S11 cells were maintained in complete RPMI 1640 medium supplemented with 10% fetal calf serum, 100 U/ml penicillin, 100 mg/ml streptomycin, 2 mM L-glutamine, and 50 mM 2-mercaptoethanol. HE2.1 cells were cultured under 300-μg/ml hygromycin selection, as previously described (46). Parental viruses include BAC-derived wild-type MHV68 (86) and the wild-type MHV68.ORF73βla (47), a recombinant marker virus that was created on the BAC-derived wild-type MHV68 backbone. All virus stocks were propagated on NIH 3T12 fibroblasts.

Generation of MHV68.ZT6 MHV68.Zt6 was generated in three stages using two-step Red-mediated recombination (49) onto the wild-type MHV68.ORF73βla (47) BAC backbone. First, a PolIII termination sequence (TTTTTT) was inserted in TMER6 at nucleotide 3749 (NC_001826.2), immediately downstream of vtRNA6 and upstream of the pre-miRNA stem loops. PAGE-purified primers homologous to sequence upstream and downstream of the TTTTTT insertion were used to amplify the I-Sce site and kanamycin resistance gene from the Kan plasmid template. The resulting amplicon was purified and electroporated into GST1783 *Escherichia coli* cells containing the MHV68.ORF73βla BAC and Red recombinase machinery. Transformed cells were grown at 30°C overnight on Kan selection, and DNA from the resulting colonies was isolated and digested with XhoI to screen for the insertion. Clones were further analyzed by pulsed-field gel electrophoresis to confirm genomic integrity. In positive clones, I-Sce was induced by incubation for 2 h in 1% arabinose to induce the second recombination. Resulting colonies were screened by PCR and PFGE. In the second stage, stem-loop deletions in TMER1, TMER2, TMER3, TMER4, and TMER5 were generated and introduced into the TMER6.stop mutant BAC. Individual TMER stem-loop miRNA mutants were cloned into pSP73 using a GeneArt seamless cloning kit (Life Technologies) and confirmed by sequencing. Following NheI digest, the TMER1-TMER5 fragment was electroporated into *E. coli* GST1783 containing the TMER6.stop mutant and recombined as described above. In the final stage, individual TMER7 and TMER8 stem-loop deletions were generated and cloned into pSP73 and then confirmed by sequencing. The TMER7-TMER8 fragment was then amplified by PCR and electroporated into *E. coli* GST173 containing the MHV68.tRNA1-tRNA5.tRNA6.stop mutant BAC. Following two-step recombination, positive clones were identified by restriction digestion and PFGE and then sequenced to confirm sequence of the mutated region. BAC DNA from the positive clone MHV68.Zt6 was isolated with a Qiagen large-construct kit and transfected into NIH 3T12 cells using a TransIT-3T3 transfection kit (MirusBio). The resulting virus was used to infect NIH 3T12 cells expressing Cre recombinase at an MOI of 0.05 to remove the BAC cassette. Titers of final viral stocks were determined by plaque assay on NIH 3T12 cells. Following generation of virus stocks, viral DNA was purified and sequenced on an Illumina GAIIx genome analyzer. The assembled sequence contig contained all anticipated mutations but otherwise displayed no other sequence deviations from the parental wild-type BAC-derived virus.

Mice and infections Female C57BL6/J mice were purchased from Jackson Laboratory (Bar Harbor, ME) at 7 to 8 weeks and were housed in a biosafety level 2+ (BSL2+) facility at the University of Florida, Gainesville, FL, in accordance with all federal guidelines and as approved by University of Florida Institutional Animal Care & Use Committee. For all C57BL6/J infections, mice were anesthetized with isoflurane and then inoculated intranasally (i.n.) with 100 or 10^4 PFU virus in 30 μl serum-free DMEM. Groups of four mice per time point, per experiment, were used for all studies. IFN-$\gamma^{-/-}$ mice on a BALB/c background [strain C.129S7(B6)$^{Ifngtm1Ts/J}$; Jackson Laboratory] were bred and housed at the University of Colorado School of Medicine, Aurora, CO, in accordance with all federal and university guidelines. BALB/c.IFN$\gamma^{-/-}$ mice ≥8 weeks of age were infected i.n. with 4×10^5 PFU of virus.

RNA isolation and stem-loop qRT-PCR. For all stem-loop qRT-PCR assays, 2×10^6 NIH 3T12 fibroblasts, S11 B cells, HE2.1 B cells, or splenocytes from infected mice were lysed using a TaqMan microRNA Cells-to-C_T kit (Applied Biosystems). Following lysis, 5 μl of sample was added to a reverse transcriptase (RT) reaction. RT reactions for individual mature miRNAs were carried out using the appropriate custom stem-loop primer, as provided in the custom TaqMan small-RNA assay. Stem-loop primers were designed using mature MHV68 miRNA sequences detailed on miRBase 19.0 (44) and in previous publications (37, 38). PCR was performed using 1.33 μl of the RT reaction mixture with 17.67 μl of the TaqMan PCR master mix with no UNG and 1 μl of the corresponding mature miRNA TaqMan probe, according to manufacturer's instructions. A copy number standard curve for mature mghv-M1-2-5p was generated using a synthetic miRIDIAN microRNA mimic (Thermo Scientific) and a suitable TaqMan probe.

Plaque assays. Plaque assays were used to determine the tissue titers during the acute phase of infection. C57BL6/J mice were infected with MHV68.ORF73βla or MHV68.ZT6, and at the indicated time points, lungs were harvested from four mice per sample group per experiment.

Plaque assays were then performed as previously described (87, 88). Briefly, harvested lung tissues were placed in sterile 2-ml screw-cap tubes containing 1 ml of DMEM and 500 μl of 1-mm zirconia-silica beads (BioSpec Products) and stored at −80°C until use. Samples were thawed on ice, and tissues were homogenized using a mini-BeadBeater (BioSpec). Samples were serially 10-fold diluted in complete DMEM, added to single wells of a 6-well plate containing a monolayer of NIH 3T12 fibroblasts, and then overlaid with methylcellulose (Sigma). After 7 days, plaques were visualized by neutral red stain and counted.

Limiting-dilution nested-PCR analysis. Single-copy-sensitive nested PCR was used to determine the frequency of cells harboring the viral genome, as previously described (47, 54). C57BL6/J mice were infected with MHV68.ORF73βla or MHV68.ZT6, and at various time points, spleens from four mice per sample group per experiment were harvested and pooled. Splenocytes were isolated, resuspended in isotonic buffer, and then serially diluted 3-fold in a background of uninfected RAW 264.7 murine macrophages, such that a total of 10^4 cells were present in each PCR. Cell dilutions and controls were then plated in a 96-well PCR plate at 12 reactions per cell dilution. Positive control reaction mixtures contained either 10, 1, or 0.1 copy of an MHV68 ORF72 plasmid in a background of RAW 264.7 cells. Negative-control reaction mixtures contained 10^4 RAW 267.4 cells only. Cells were lysed using proteinase K for 8 h at 56°C. Following enzyme inactivation, nested PCR was performed using primers specific for MHV68 ORF72, as previously described (54). Reactions positive for viral genome resulted in a 195-bp amplicon, which was visualized on a 3% agarose gel with ethidium bromide.

Limiting-dilution *ex vivo* reactivation and preformed-virus analyses. The limiting-dilution assays were used to determine the frequency of cells that spontaneously reactivate from latency *ex vivo* or that contain preformed infectious virus particles (48, 58). C57BL6/J mice were infected with MHV68.ORF73βla or MHV68.ZT6, and at various time points, spleens from four mice per sample group per experiment were harvested and pooled. Splenocytes were isolated and resuspended in complete DMEM at 10^6 cells per ml. Cells were plated in 2-fold serial dilution in a 96-well tissue culture plate over a monolayer of MEFs (24 wells per cell dilution). Wells were scored for cytopathic effect (CPE) at 21 days. To detect preformed virus, parallel samples were mechanically disrupted, which destroys cells, and therefore eliminates the possibility of reactivation from latency, but does not damage intact virus particles (48). Disrupted samples were then 2-fold serially diluted, plated over a monolayer of MEFs (24 wells per cell dilution), and scored for CPE at 21 days.

Flow cytometry. Flow cytometry was used to determine the cell surface phenotype of infected splenocytes expressing the β-lactamase marker, as previously described (47). C57BL6/J mice were infected with MHV68.ORF73βla or MHV68.ZT6, and at various time points, spleens from four mice per sample group per experiment were harvested and pooled. Following splenocyte isolation and red blood cell lysis, samples were blocked in fluorescence-activated cell sorting (FACS) buffer containing purified anti-mouse CD16/CD32 (Fc block). Cells were then stained with rat anti-mouse CD19-APC/Cy7 (clone ID3; BD Biosciences), IgM-APC (clone II/41; BD Biosciences), and CD38 AlexaFluor700 (clone 90; eBiosciences). In some experiments, biotinylated peanut agglutinin (Vector Labs) followed by streptavidin-AlexaFluor700 (Life Technologies) was used in place of CD38 staining. Following cell surface staining, cells were washed twice and then resuspended in staining buffer containing freshly prepared CCF4-AM β-lactamase substrate (LiveBLAzer FRET B/G reagent; Life Technologies) for 1 h. Cells were then washed twice, resuspended in phosphate-buffered saline (PBS), and kept on ice until processing. Unstained, fluorescence-minus-one, and isotype-stained controls were also included in each experiment. A BD LSR II flow cytometer was used to collect sample data using the following scheme: developing B cells ($CD19^+$ $AA4^+$), naive follicular B cells ($CD19^+$ IgM^+), mature B cells ($CD19^+$ $AA4^-$), germinal-center B cells ($CD19^+$ IgM^- $CD38^{low/-}$ or $CD19^+$ IgM^- PNA^+), and memory B cells ($CD19^+$ IgM^- $CD38^+$ or $CD19^+$ IgM^- $PNA^{low/-}$). Data were analyzed using FlowJo software (Tree Star).

Statistical analysis. All data were analyzed using GraphPad Prism software (GraphPad Software, San Diego, CA). The percentages of β-lactamase-positive B cell subsets were statistically analyzed using a one-way unpaired Student's *t* test. The frequencies of viral genome-positive cells were determined from the nonlinear regression analysis of sigmoidal dose-response curve data. Based on Poisson distributions, the frequency at which at least one event in a given population is present occurs at the point where the regression analysis line intersects 63.2%.

SUPPLEMENTAL MATERIAL

Supplemental material for this article may be found at http://mbio.asm.org/lookup/suppl/doi:10.1128/mBio.00981-14/-/DCSupplemental.

Figure S1, PDF file, 0.1 MB.
Figure S2, PDF file, 0.1 MB.
Figure S3, PDF file, 2.1 MB.
Figure S4, PDF file, 0.1 MB.
Table S1, PDF file, 0.1 MB.
Table S2, PDF file, 0.1 MB.
Table S3, PDF file, 0.1 MB.

REFERENCES

1. **Cesarman E.** 2011. Gammaherpesvirus and lymphoproliferative disorders in immunocompromised patients. Cancer Lett. **305:**163–174. http://dx.doi.org/10.1016/j.canlet.2011.03.003.
2. **Mesri EA, Cesarman E, Boshoff C.** 2010. Kaposi's sarcoma and its associated herpesvirus. Nat. Rev. Cancer **10:**707–719. http://dx.doi.org/10.1038/nrc2888.
3. **Kutok JL, Wang F.** 2006. Spectrum of Epstein-Barr virus–associated diseases. Annu. Rev. Pathol. Mech. Dis. **1:**375–404. http://dx.doi.org/10.1146/annurev.pathol.1.110304.100209.
4. **Babcock GJ, Decker LL, Volk M, Thorley-Lawson DA.** 1998. EBV persistence in memory B cells *in vivo*. Immunity **9:**395–404. http://dx.doi.org/10.1016/S1074-7613(00)80622-6.
5. **Willer DO, Speck SH.** 2003. Long-term latent murine gammaherpesvirus 68 infection is preferentially found within the surface immunoglobulin D-negative subset of splenic B cells *in vivo*. J. Virol. **77:**8310–8321. http://dx.doi.org/10.1128/JVI.77.15.8310-8321.2003.
6. **Sunil-Chandra NP, Efstathiou S, Nash AA.** 1992. Murine gammaherpesvirus 68 establishes a latent infection in mouse B lymphocytes *in vivo*. J. Gen. Virol. **73:**3275–3279. http://dx.doi.org/10.1099/0022-1317-73-12-3275.
7. **Flaño E, Kim IJ, Woodland DL, Blackman MA.** 2002. Gammaherpesvirus latency is preferentially maintained in splenic germinal center and memory B cells. J. Exp. Med. **196:**1363–1372. http://dx.doi.org/10.1084/jem.20020890.
8. **Harrington WJ, Bagasra O, Sosa CE, Bobroski LE, Baum M, Wen XL, Cabral L, Byrne GE, Pomerantz RJ, Wood C.** 1996. Human herpesvirus type 8 DNA sequences in cell-free plasma and mononuclear cells of Kaposi's sarcoma patients. J. Infect. Dis. **174:**1101–1105. http://dx.doi.org/10.1093/infdis/174.5.1101.
9. **Ambroziak JA, Blackbourn DJ, Herndier BG, Glogau RG, Gullett JH, McDonald AR, Lennette ET, Levy JA.** 1995. Herpes-like sequences in HIV-infected and uninfected Kaposi's sarcoma patients. Science **268:**582–583. http://dx.doi.org/10.1126/science.7725108.
10. **Pfeffer S, Zavolan M, Grässer FA, Chien M, Russo JJ, Ju J, John B, Enright AJ, Marks D, Sander C, Tuschl T.** 2004. Identification of virus-encoded microRNAs. Science **304:**734–736. http://dx.doi.org/10.1126/science.1096781.
11. **Pfeffer S, Sewer A, Lagos-Quintana M, Sheridan R, Sander C, Grässer FA, van Dyk LF, Ho CK, Shuman S, Chien M, Russo JJ, Ju J, Randall G, Lindenbach BD, Rice CM, Simon V, Ho DD, Zavolan M, Tuschl T.** 2005. Identification of microRNAs of the herpesvirus family. Nat. Methods **2:**269–276. http://dx.doi.org/10.1038/nmeth746.
12. **Bartel DP.** 2009. MicroRNAs: target recognition and regulatory functions. Cell **136:**215–233. http://dx.doi.org/10.1016/j.cell.2009.01.002.
13. **Kincaid RP, Sullivan CS.** 2012. Virus-encoded microRNAs: an overview and a look to the future. PLoS Pathog. **8:**e1003018. http://dx.doi.org/10.1371/journal.ppat.1003018.

14. **Grundhoff A, Sullivan CS.** 2011. Virus-encoded microRNAs. Virology **411:**325–343. http://dx.doi.org/10.1016/j.virol.2011.01.002.
15. **Cullen BR.** 2011. Viruses and microRNAs: RISCy interactions with serious consequences. Genes Dev. **25:**1881–1894. http://dx.doi.org/10.1101/gad.17352611.
16. **Zhu Y, Haecker I, Yang Y, Gao SJ, Renne R.** 2013. γ-Herpesvirus-encoded miRNAs and their roles in viral biology and pathogenesis. Curr. Opin. Virol. **3:**266–275. http://dx.doi.org/10.1016/j.coviro.2013.05.013.
17. **Cai X, Schäfer A, Lu S, Bilello JP, Desrosiers RC, Edwards R, Raab-Traub N, Cullen BR.** 2006. Epstein-Barr virus microRNAs are evolutionarily conserved and differentially expressed. PLoS Pathog. **2:**e23. http://dx.doi.org/10.1371/journal.ppat.0020023.
18. **Grundhoff A, Sullivan CS, Ganem D.** 2006. A combined computational and microarray-based approach identifies novel microRNAs encoded by human gamma-herpesviruses. RNA **12:**733–750. http://dx.doi.org/10.1261/rna.2326106.
19. **Samols MA, Hu J, Skalsky RL, Renne R.** 2005. Cloning and identification of a MicroRNA cluster within the latency-associated region of Kaposi's sarcoma-associated herpesvirus. J. Virol. **79:**9301–9305. http://dx.doi.org/10.1128/JVI.79.14.9301-9305.2005.
20. **Cai X, Lu S, Zhang Z, Gonzalez CM, Damania B, Cullen BR.** 2005. Kaposi's sarcoma-associated herpesvirus expresses an array of viral microRNAs in latently infected cells. Proc. Natl. Acad. Sci. U. S. A. **102:**5570–5575. http://dx.doi.org/10.1073/pnas.0408192102.
21. **Dölken L, Malterer G, Erhard F, Kothe S, Friedel CC, Suffert G, Marcinowski L, Motsch N, Barth S, Beitzinger M, Lieber D, Bailer SM, Hoffmann R, Ruzsics Z, Kremmer E, Pfeffer S, Zimmer R, Koszinowski UH, Grässer F, Meister G, Haas J.** 2010. Systematic analysis of viral and cellular microRNA targets in cells latently infected with human γ-herpesviruses by RISC immunoprecipitation assay. Cell Host Microbe **7:**324–334. http://dx.doi.org/10.1016/j.chom.2010.03.008.
22. **Riley KJ, Rabinowitz GS, Yario TA, Luna JM, Darnell RB, Steitz JA.** 2012. EBV and human microRNAs co-target oncogenic and apoptotic viral and human genes during latency. EMBO J. **31:**2207–2221. http://dx.doi.org/10.1038/emboj.2012.63.
23. **Skalsky RL, Corcoran DL, Gottwein E, Frank CL, Kang D, Hafner M, Nusbaum JD, Feederle R, Delecluse HJ, Luftig MA, Tuschl T, Ohler U, Cullen BR.** 2012. The viral and cellular microRNA targetome in lymphoblastoid cell lines. PLoS Pathog. **8:**e1002484. http://dx.doi.org/10.1371/journal.ppat.1002484.
24. **Gottwein E, Corcoran DL, Mukherjee N, Skalsky RL, Hafner M, Nusbaum JD, Shamulailatpam P, Love CL, Dave SS, Tuschl T, Ohler U, Cullen BR.** 2011. Viral microRNA targetome of KSHV-infected primary effusion lymphoma cell lines. Cell Host Microbe **10:**515–526. http://dx.doi.org/10.1016/j.chom.2011.09.012.
25. **Haecker I, Gay LA, Yang Y, Hu J, Morse AM, McIntyre LM, Renne R.** 2012. Ago HITS-CLIP expands understanding of Kaposi's sarcoma-associated herpesvirus miRNA function in primary effusion lymphomas. PLoS Pathog. **8:**e1002884. http://dx.doi.org/10.1371/journal.ppat.1002884.
26. **Ramalingam D, Kieffer-Kwon P, Ziegelbauer JM.** 2012. Emerging themes from EBV and KSHV microRNA targets. Viruses **4:**1687–1710. http://dx.doi.org/10.3390/v4091687.
27. **Gottwein E, Mukherjee N, Sachse C, Frenzel C, Majoros WH, Chi JT, Braich R, Manoharan M, Soutschek J, Ohler U, Cullen BR.** 2007. A viral microRNA functions as an orthologue of cellular miR-155. Nature **450:**1096–1099. http://dx.doi.org/10.1038/nature05992.
28. **Skalsky RL, Samols MA, Plaisance KB, Boss IW, Riva A, Lopez MC, Baker HV, Renne R.** 2007. Kaposi's sarcoma-associated herpesvirus encodes an ortholog of miR-155. J. Virol. **81:**12836–12845. http://dx.doi.org/10.1128/JVI.01804-07.
29. **Dahlke C, Maul K, Christalla T, Walz N, Schult P, Stocking C, Grundhoff A.** 2012. A microRNA encoded by Kaposi sarcoma-associated herpesvirus promotes B-cell expansion *in vivo*. PLoS One **7:**e49435. http://dx.doi.org/10.1371/journal.pone.0049435.
30. **Boss IW, Nadeau PE, Abbott JR, Yang Y, Mergia A, Renne R.** 2011. A Kaposi's sarcoma-associated herpesvirus-encoded ortholog of microRNA miR-155 induces human splenic B-cell expansion in NOD/LtSz-scid IL2Rγnull mice. J. Virol. **85:**9877–9886. http://dx.doi.org/10.1128/JVI.05558-11.
31. **Cazalla D, Yario T, Steitz JA, Steitz J.** 2010. Down-regulation of a host microRNA by a herpesvirus Saimiri noncoding RNA. Science **328:**1563–1566. http://dx.doi.org/10.1126/science.1187197.
32. **Barton E, Mandal P, Speck SH.** 2011. Pathogenesis and host control of gammaherpesviruses: lessons from the mouse. Annu. Rev. Immunol. **29:**351–397. http://dx.doi.org/10.1146/annurev-immunol-072710-081639.
33. **Virgin HW IV, Latreille P, Wamsley P, Hallsworth K, Weck KE, Dal Canto AJ, Speck SH.** 1997. Complete sequence and genomic analysis of murine gammaherpesvirus 68. J. Virol. **71:**5894–5904.
34. **Blaskovic D, Stanceková M, Svobodová J, Mistríková J.** 1980. Isolation of five strains of herpesviruses from two species of free living small rodents. Acta Virol. **24:**468.
35. **Sunil-Chandra NP, Arno J, Fazakerley J, Nash AA.** 1994. Lymphoproliferative disease in mice infected with murine gammaherpesvirus 68. Am. J. Pathol. **145:**818–826.
36. **Tarakanova VL, Suarez F, Tibbetts SA, Jacoby MA, Weck KE, Hess JL, Speck SH, Virgin HW.** 2005. Murine gammaherpesvirus 68 infection is associated with lymphoproliferative disease and lymphoma in BALB {beta}2 microglobulin-deficient mice. J. Virol. **79:**14668–14679. http://dx.doi.org/10.1128/JVI.79.23.14668-14679.2005.
37. **Reese TA, Xia J, Johnson LS, Zhou X, Zhang W, Virgin HW.** 2010. Identification of novel microRNA-like molecules generated from herpesvirus and host tRNA transcripts. J. Virol. **84:**10344–10353. http://dx.doi.org/10.1128/JVI.00707-10.
38. **Zhu JY, Strehle M, Frohn A, Kremmer E, Höfig KP, Meister G, Adler H.** 2010. Identification and analysis of expression of novel microRNAs of murine gammaherpesvirus 68. J. Virol. **84:**10266–10275. http://dx.doi.org/10.1128/JVI.01119-10.
39. **Xia J, Zhang W.** 2012. Noncanonical microRNAs and endogenous siRNAs in lytic infection of murine gammaherpesvirus. PLoS One **7:**e47863. http://dx.doi.org/10.1371/journal.pone.0047863.
40. **Bogerd HP, Karnowski HW, Cai X, Shin J, Pohlers M, Cullen BR.** 2010. A mammalian herpesvirus uses noncanonical expression and processing mechanisms to generate viral MicroRNAs. Mol. Cell **37:**135–142. http://dx.doi.org/10.1016/j.molcel.2009.12.016.
41. **Diebel KW, Smith AL, van Dyk LF.** 2010. Mature and functional viral miRNAs transcribed from novel RNA polymerase III promoters. RNA **16:**170–185. http://dx.doi.org/10.1261/rna.1873910.
42. **Bowden RJ, Simas JP, Davis AJ, Efstathiou S.** 1997. Murine gammaherpesvirus 68 encodes tRNA-like sequences which are expressed during latency. J. Gen. Virol. **78:**1675–1687.
43. **Xia J, Zhang W.** 2012. Noncanonical microRNAs and endogenous siRNAs in lytic infection of murine gammaherpesvirus. PLoS One **7:**e47863. http://dx.doi.org/10.1371/journal.pone.0047863.
44. **Kozomara A, Griffiths-Jones S.** 2011. miRBase: integrating microRNA annotation and deep-sequencing data. Nucleic Acids Res. **39:**D152–D157. http://dx.doi.org/10.1093/nar/gkq1027.
45. **Usherwood EJ, Stewart JP, Nash AA.** 1996. Characterization of tumor cell lines derived from murine gammaherpesvirus-68-infected mice. J. Virol. **70:**6516–6518.
46. **Forrest JC, Speck SH.** 2008. Establishment of B-cell lines latently infected with reactivation-competent murine gammaherpesvirus 68 provides evidence for viral alteration of a DNA damage-signaling cascade. J. Virol. **82:**7688–7699. http://dx.doi.org/10.1128/JVI.02689-07.
47. **Nealy MS, Coleman CB, Li H, Tibbetts SA.** 2010. Use of a virus-encoded enzymatic marker reveals that a stable fraction of memory B cells expresses latency-associated nuclear antigen throughout chronic gammaherpesvirus Infection. J. Virol. **84:**7523–7534. http://dx.doi.org/10.1128/JVI.02572-09.
48. **Weck KE, Kim SS, Virgin HW, Speck SH.** 1999. B cells regulate murine gammaherpesvirus 68 latency. J. Virol. **73:**4651–4661.
49. **Tischer BK, von Einem J, Kaufer B, Osterrieder N.** 2006. Two-step red-mediated recombination for versatile high-efficiency markerless DNA manipulation in Escherichia coli. BioTechniques **40:**191–197. http://dx.doi.org/10.2144/000112096.
50. **Coleman CB, Nealy MS, Tibbetts SA.** 2010. Immature and transitional B cells are latency reservoirs for a gammaherpesvirus. J. Virol. **84:**13045–13052. http://dx.doi.org/10.1128/JVI.01455-10.
51. **Zuker M.** 2003. Mfold web server for nucleic acid folding and hybridization prediction. Nucleic Acids Res. **31:**3406–3415. http://dx.doi.org/10.1093/nar/gkg595.
52. **Jacoby MA, Virgin HW, Speck SH.** 2002. Disruption of the M2 gene of murine gammaherpesvirus 68 alters splenic latency following intranasal, but not intraperitoneal, inoculation. J. Virol. **76:**1790–1801. http://dx.doi.org/10.1128/JVI.76.4.1790-1801.2002.
53. **Simas JP, Marques S, Bridgeman A, Efstathiou S, Adler H.** 2004. The

M2 gene product of murine gammaherpesvirus 68 is required for efficient colonization of splenic follicles but is not necessary for expansion of latently infected germinal centre B cells. J. Gen. Virol. **85:**2789–2797. http://dx.doi.org/10.1099/vir.0.80138-0.

54. **Tibbetts SA, McClellan JS, Gangappa S, Speck SH, Virgin HW.** 2003. Effective vaccination against long-term gammaherpesvirus latency. J. Virol. **77:**2522–2529. http://dx.doi.org/10.1128/JVI.77.4.2522-2529.2003.
55. **Ridderstad A, Tarlinton DM.** 1998. Kinetics of establishing the memory B cell population as revealed by CD38 expression. J. Immunol. **160:**4688–4695.
56. **Shinall SM, Gonzalez-Fernandez M, Noelle RJ, Waldschmidt TJ.** 2000. Identification of murine germinal center B cell subsets defined by the expression of surface isotypes and differentiation antigens. J. Immunol. **164:**5729–5738. http://dx.doi.org/10.4049/jimmunol.164.11.5729.
57. **Stevenson PG, Simas JP, Efstathiou S.** 2009. Immune control of mammalian gamma-herpesviruses: lessons from murid herpesvirus-4. J. Gen. Virol. **90:**2317–2330. http://dx.doi.org/10.1099/vir.0.013300-0.
58. **Tibbetts SA, van Dyk LF, Speck SH, Virgin HW.** 2002. Immune control of the number and reactivation phenotype of cells latently infected with a gammaherpesvirus. J. Virol. **76:**7125–7132. http://dx.doi.org/10.1128/JVI.76.14.7125-7132.2002.
59. **Gangappa S, van Dyk LF, Jewett TJ, Speck SH, Virgin HW.** 2002. Identification of the *in vivo* role of a viral bcl-2. J. Exp. Med. **195:**931–940. http://dx.doi.org/10.1084/jem.20011825.
60. **Weck KE, Dal Canto AJ, Gould JD, O'Guin AK, Roth KA, Saffitz JE, Speck SH, Virgin HW.** 1997. Murine gamma-herpesvirus 68 causes severe large-vessel arteritis in mice lacking interferon-gamma responsiveness: a new model for virus-induced vascular disease. Nat. Med. **3:**1346–1353. http://dx.doi.org/10.1038/nm1297-1346.
61. **Mora AL, Woods CR, Garcia A, Xu J, Rojas M, Speck SH, Roman J, Brigham KL, Stecenko AA.** 2005. Lung infection with γ-herpesvirus induces progressive pulmonary fibrosis in Th2-biased mice. Am. J. Physiol. Lung Cell. Mol. Physiol. **289:**L711–L721. http://dx.doi.org/10.1152/ajplung.00007.2005.
62. **Lee KS, Groshong SD, Cool CD, Kleinschmidt-DeMasters BK, van Dyk LF.** 2009. Murine gammaherpesvirus 68 infection of IFNγ unresponsive mice: a small animal model for gammaherpesvirus-associated B-cell lymphoproliferative disease. Cancer Res. **69:**5481–5489. http://dx.doi.org/10.1158/0008-5472.CAN-09-0291.
63. **Lee KS, Cool CD, van Dyk LF.** 2009. Murine gammaherpesvirus 68 infection of gamma interferon-deficient mice on a BALB/c background Results in acute lethal pneumonia that is dependent on specific viral genes. J. Virol. **83:**11397–11401. http://dx.doi.org/10.1128/JVI.00989-09.
64. **Dölken L, Perot J, Cognat V, Alioua A, John M, Soutschek J, Ruzsics Z, Koszinowski U, Voinnet O, Pfeffer S.** 2007. Mouse cytomegalovirus microRNAs dominate the cellular small RNA profile during lytic infection and show features of posttranscriptional regulation. J. Virol. **81:**13771–13782. http://dx.doi.org/10.1128/JVI.01313-07.
65. **Michlewski G, Guil S, Semple CA, Cáceres JF.** 2008. Posttranscriptional regulation of miRNAs harboring conserved terminal loops. Mol. Cell **32:**383–393. http://dx.doi.org/10.1016/j.molcel.2008.10.013.
66. **Kai ZS, Pasquinelli AE.** 2010. MicroRNA assassins: factors that regulate the disappearance of miRNAs. Nat. Struct. Mol. Biol. **17:**5–10. http://dx.doi.org/10.1038/nsmb.1762.
67. **Chatterjee S, Grosshans H.** 2009. Active turnover modulates mature microRNA activity in Caenorhabditis elegans. Nature **461:**546–549. http://dx.doi.org/10.1038/nature08349.
68. **Umbach JL, Cullen BR.** 2010. In-depth analysis of Kaposi's sarcoma-associated herpesvirus microRNA expression provides insights into the mammalian microRNA-processing machinery. J. Virol. **84:**695–703. http://dx.doi.org/10.1128/JVI.02013-09.
69. **Macrae AI, Dutia BM, Milligan S, Brownstein DG, Allen DJ, Mistrikova J, Davison AJ, Nash AA, Stewart JP.** 2001. Analysis of a novel strain of murine gammaherpesvirus reveals a genomic locus important for acute pathogenesis. J. Virol. **75:**5315–5327.
70. **Clambey ET, Virgin HW, Speck SH.** 2002. Characterization of a spontaneous 9.5-kilobase-deletion mutant of murine gammaherpesvirus 68 reveals tissue-specific genetic requirements for latency. J. Virol. **76:**6532–6544.
71. **Ebert MS, Sharp PA.** 2012. Roles for microRNAs in conferring robustness to biological processes. Cell **149:**515–524. http://dx.doi.org/10.1016/j.cell.2012.04.005.
72. **Thorley-Lawson DA, Gross A.** 2004. Persistence of the Epstein-Barr virus and the origins of associated lymphomas. N. Engl. J. Med. **350:**1328–1337. http://dx.doi.org/10.1056/NEJMra032015.
73. **Macrae AI, Usherwood EJ, Husain SM, Flano E, Kim IJ, Woodland DL, Nash AA, Blackman MA, Sample JT, Stewart JP.** 2003. Murid herpesvirus 4 strain 68 M2 protein is a B-cell-associated antigen important for latency but not lymphocytosis. J. Virol. **77:**9700–9709. http://dx.doi.org/10.1128/JVI.77.17.9700-9709.2003.
74. **Fleming HE, Milne CD, Paige CJ.** 2004. CD45-deficient mice accumulate pro-B cells both *in vivo* and *in vitro*. J. Immunol. **173:**2542–2551.
75. **Zhao Y, Xu H, Yao Y, Smith LP, Kgosana L, Green J, Petherbridge L, Baijent SJ, Nair V.** 2011. Critical role of the virus-encoded microRNA-155 ortholog in the induction of Marek's disease lymphomas. PLoS Pathog. **7:**e1001305. http://dx.doi.org/10.1371/journal.ppat.1001305.
76. **Marshall V, Parks T, Bagni R, Wang CD, Samols MA, Hu J, Wyvil KM, Aleman K, Little RF, Yarchoan R, Renne R, Whitby D.** 2007. Conservation of virally encoded microRNAs in Kaposi sarcoma-associated herpesvirus in primary effusion lymphoma cell lines and in patients with Kaposi sarcoma or multicentric Castleman disease. J. Infect. Dis. **195:**645–659. http://dx.doi.org/10.1086/511434.
77. **Chugh PE, Sin SH, Ozgur S, Henry DH, Menezes P, Griffith J, Eron JJ, Damania B, Dittmer DP.** 2013. Systemically circulating viral and tumor-derived microRNAs in KSHV-associated malignancies. PLoS Pathog. **9:**e1003484. http://dx.doi.org/10.1371/journal.ppat.1003484.
78. **Cosmopoulos K, Pegtel M, Hawkins J, Moffett H, Novina C, Middeldorp J, Thorley-Lawson DA.** 2009. Comprehensive profiling of Epstein-Barr virus microRNAs in nasopharyngeal carcinoma. J. Virol. **83:**2357–2367. http://dx.doi.org/10.1128/JVI.02104-08.
79. **Imig J, Motsch N, Zhu JY, Barth S, Okoniewski M, Reineke T, Tinguely M, Faggioni A, Trivedi P, Meister G, Renner C, Grässer FA.** 2011. MicroRNA profiling in Epstein-Barr virus-associated B-cell lymphoma. Nucleic Acids Res. **39:**1880–1893. http://dx.doi.org/10.1093/nar/gkq1043.
80. **Fabbri M, Paone A, Calore F, Galli R, Gaudio E, Santhanam R, Lovat F, Fadda P, Mao C, Nuovo GJ, Zanesi N, Crawford M, Ozer GH, Wernicke D, Alder H, Caligiuri MA, Nana-Sinkam P, Perrotti D, Croce CM.** 2012. MicroRNAs bind to Toll-like receptors to induce prometastatic inflammatory response. Proc. Natl. Acad. Sci. U. S. A. **109** 201209414. http://dx.doi.org/10.1073/pnas.1209414109.
81. **Weck KE, Kim SS, Virgin HW, Speck SH.** 1999. Macrophages are the major reservoir of latent murine gammaherpesvirus 68 in peritoneal cells. J. Virol. **73:**3273–3283.
82. **Murphy E, Vaníček J, Robins H, Shenk T, Levine AJ.** 2008. Suppression of immediate-early viral gene expression by herpesvirus-coded microRNAs: implications for latency. Proc. Natl. Acad. Sci. U. S. A. **105:**5453–5458. http://dx.doi.org/10.1073/pnas.0711910105.
83. **Lin X, Liang D, He Z, Deng Q, Robertson ES, Lan K.** 2011. miR-K12-7-5p encoded by Kaposi's sarcoma-associated herpesvirus stabilizes the latent state by targeting viral ORF50/RTA. PLoS One **6:**e16224. http://dx.doi.org/10.1371/journal.pone.0016224.
84. **Bellare P, Ganem D.** 2009. Regulation of KSHV lytic switch protein expression by a virus-encoded microRNA: an evolutionary adaptation that fine-tunes lytic reactivation. Cell Host Microbe **6:**570–575. http://dx.doi.org/10.1016/j.chom.2009.11.008.
85. **Lu CC, Li Z, Chu CY, Feng J, Feng J, Sun R, Rana TM.** 2010. MicroRNAs encoded by Kaposi's sarcoma-associated herpesvirus regulate viral life cycle. EMBO Rep. **11:**784–790. http://dx.doi.org/10.1038/embor.2010.132.
86. **Adler H, Messerle M, Wagner M, Koszinowski UH.** 2000. Cloning and mutagenesis of the murine gammaherpesvirus 68 genome as an infectious bacterial artificial chromosome. J. Virol. **74:**6964–6974. http://dx.doi.org/10.1128/JVI.74.15.6964-6974.2000.
87. **Van Dyk LF, Virgin HW, Speck SH.** 2000. The murine gammaherpesvirus 68 v-cyclin is a critical regulator of reactivation from latency. J. Virol. **74:**7451–7461. http://dx.doi.org/10.1128/JVI.74.16.7451-7461.2000.
88. **Van Berkel V, Levine B, Kapadia SB, Goldman JE, Speck SH, Virgin HW.** 2002. Critical role for a high-affinity chemokine-binding protein in γ-herpesvirus-induced lethal meningitis. J. Clin. Invest. **109:**905–914. http://dx.doi.org/10.1172/JCI14358.